PTEP

Prog. Theor. Exp. Phys. **2015**, 013B02 (33 pages)
DOI: 10.1093/ptep/ptu168

Anomalous radiative transitions

Kenzo Ishikawa[1,*], Toshiki Tajima[2,3,*], and Yutaka Tobita[1,*]

[1]*Department of Physics, Faculty of Science, Hokkaido University, Sapporo 060-0810, Japan*
[2]*Department of Physics and Astronomy, University of California, Irvine, CA 92697, USA*
[3]*KEK High Energy Accelerator Research Organization, Tsukuba 305-0801, Japan*
[*]E-mail: ishikawa@particle.sci.hokudai.ac.jp, ttajima@uci.edu, tobita@particle.sci.hokudai.ac.jp

Received September 30, 2014; Accepted November 9, 2014; Published January 1, 2015

Anomalous transitions involving photons derived by many-body interaction of the form $\partial_\mu G^\mu$ in the standard model are studied for the first time. This does not affect the equation of motion in the bulk, but modifies the wavefunctions, and causes an unusual transition characterized by a time-independent probability. In the transition probability at a time interval T expressed generally in the form $P = T\Gamma_0 + P^{(d)}$, now with $P^{(d)} \neq 0$. The diffractive term $P^{(d)}$ has its origin in the overlap of waves of the initial and final states, and reveals the characteristics of waves. In particular, the processes of the neutrino–photon interaction ordinarily forbidden by the Landau–Yang theorem ($\Gamma_0 = 0$) manifest themselves through the boundary interaction. The new term leads physical processes over a wide energy range to have finite probabilities. New methods of detecting neutrinos using lasers are proposed, based on this diffractive term; these would enhance the detectability of neutrinos by many orders of magnitude.

Subject Index B50, B54, B59

1. Matter waves and $S[T]$

In modern science and technology, quantum mechanics plays a fundamental role. Despite the fact that stationary phenomena and methods have been well developed, those of non-stationary phenomena have not. In the former, the de Broglie wavelength $\hbar/p$ determines a typical length and is of microscopic size, scatterings or reactions on the macroscopic scale are considered independent, and successive reactions have been treated under the independent scattering hypothesis. The probability of the event that they occur is computed by the incoherent sum of each value. In the latter, time and space variables vary simultaneously, and a new scale, which can be much larger than the de Broglie wavelength, emerges. They appear in overlapping regions of the initial and final waves, and show unique properties of intriguing quantum mechanical waves.

A transition rate computed with a method for stationary waves with initial and final states defined at the infinite-time interval $T = \infty$ is independent of the details of the wavefunctions. They hold characteristics of particles and preserve the symmetry of the system. Transitions occurring at a finite T, however, reveal characteristics of waves, the dependence on the boundary conditions [1,2][1],

[1] It was pointed out by Sakurai [3], Peierls [4], and Greiner [5] that the probability at finite T would be different from that at $T = \infty$. Hereafter we compute the difference for the detected particle that has the mean free path (mfp) $l_{\rm mfp}$ of $l_{\rm mfp} \gg cT$.

Funded by SCOAP[3]

and the probability

$$P = T\Gamma_0 + P^{(d)}, \tag{1}$$

where $P^{(d)}$ is the diffractive term, which has often escaped the attention of researchers. The rate Γ_0 is computed with Fermi's golden rule [6–10], and preserves the internal and space-time symmetries, including the kinetic-energy conservation. Γ_0 holds the characteristic properties of particles and the hypothesis of independent scatterings is valid. For a particle of small mass, m_s, $\Gamma_0(p_i, m_s)$ behaves as

$$\Gamma_0(p_i, m_s) \approx \Gamma_0(p_i, 0), \tag{2}$$

because the characteristic length, the de Broglie wavelength, is determined with p_i. The region where $P^{(d)}$ is ignorable is called the particle zone.

Overlapping waves in the initial and final states have finite interaction energy, and reveal unique properties of the waves [1,2]. Because the interaction energy is part of the total energy, sharing with the kinetic energy, the conservation law of kinetic energy is violated. Consequently, the state becomes non-uniform in time and the transition probability has a new component $P^{(d)}$, showing characteristics of waves. The term $P^{(d)}/T$ was shown to behave with a new scale of length, $(\hbar/m_s c) \times (E_i/m_s c^2)$. Accordingly, the correction is proportional to the ratio of two small quantities:

$$\frac{P^{(d)}}{T} = f\left(\frac{1/T}{m_s^2 c^3/\hbar E_i}\right), \tag{3}$$

where f is a certain function and does not follow the property of Eq. (2).

The term $P^{(d)}$ reflects the non-stationary waves and is not computed with the stationary waves. In the region where $P^{(d)}$ is important, the hypothesis of independent scattering is invalid, and interference unique to waves manifests. This region is called the wave zone, and extends to a large area for light particles. This term $P^{(d)}$ has been ignored, but yields important contributions to the probability in various processes. In particular, $P^{(d)}$ is inevitable for the process of $\Gamma_0 = 0$ and $P^{(d)} \neq 0$. This often occurs. Furthermore, $P^{(d)}$ can be drastically enhanced, if the overlap of the waves is constructive over a wide area. This happens for small m_s, large E_i, and even for large T, and pertains to macroscopic quantum phenomena. In particular, processes of large $P^{(d)}$ involving photons and neutrinos in the standard model are studied in the present paper.

As an example showing $\Gamma_0 = 0$, $P^{(d)} \neq 0$ is a system of fields described by a free part Lagrangian L_0 and interaction part $L_{\rm int}$ of total derivative,

$$L = L_0 + L_{\rm int}, \quad L_{\rm int} = \frac{d}{dt}G, \tag{4}$$

where G is a polynomial of fields $\phi_l(x)$. Here $\phi_l(x)$ follows the free equation

$$\frac{\partial L_0}{\partial \phi_l(x)} - \frac{\partial}{\partial x_\mu}\frac{\partial L_0}{\partial \frac{\partial \phi_l(x)}{\partial x_\mu}} = 0. \tag{5}$$

The interaction Lagrangian $L_{\rm int}$ decouples from the equation and does not modify the equation of motion in classical and quantum mechanics. Nevertheless, the wavefunction $|\Psi(t)\rangle$ follows the

Schrödinger equation in the interaction picture,

$$i\hbar\frac{\partial}{\partial t}|\Psi\rangle_{\rm int} = \left(\frac{\partial}{\partial t}G_{\rm int}(t)\right)|\Psi\rangle_{\rm int}, \tag{6}$$

where the free part, H_0, and the interaction part, $H_{\rm int}$, are derived from the previous Lagrangian, and $G_{\rm int}$ stands for G of the interaction picture. A solution at t,

$$|\Psi(t)\rangle_{\rm int} = e^{\frac{G_{\rm int}(t)-G_{\rm int}(0)}{i\hbar}}|\Psi(0)\rangle_{\rm int}, \tag{7}$$

is expressed with $G(t)$, and the state at $t > 0$ is modified by the interaction. The initial state $|\Psi(0)\rangle_{\rm int}$ prepared at $t = 0$ is transformed to the other state of t-independent weight. Hence, the state in Eq. (7) is like stationary, and $\Gamma_0 = 0$, and $P^{(d)} \neq 0$. Physical observables are expressed by the probability of the events, which are specified by the initial and final states. For those at finite T, the normal S-matrix, $S[\infty]$, which satisfies the boundary condition at $T = \infty$ instead of that at finite T, is useless. $S[T]$ that satisfies the boundary condition at T is necessary and has been constructed in Refs. [1,2]. $S[T]$ is applied to the system described by Eq. (4).

$S[T]$ is constructed with the Møller operators at a finite T, $\Omega_\pm(T)$, as $S[T] = \Omega_-^\dagger(T)\Omega_+(T)$. $\Omega_\pm(T)$ are expressed by a free Hamiltonian H_0 and a total Hamiltonian H by $\Omega_\pm(T) = \lim_{t\to\mp T/2} e^{iHt}e^{-iH_0t}$. From this expression, $S[T]$ is unitary and satisfies

$$[S[T], H_0] \neq 0, \tag{8}$$

hence a matrix element of $S[T]$ between two eigenstates of H_0, $|\alpha\rangle$ and $|\beta\rangle$ of eigenvalues E_α and E_β, is decomposed into two components:

$$\langle\beta|S[T]|\alpha\rangle = \left\langle\beta|S^{(n)}[T]|\alpha\right\rangle + \left\langle\beta|S^{(d)}[T]|\alpha\right\rangle, \tag{9}$$

where $\langle\beta|S^{(n)}|\alpha\rangle$ and $\langle\beta|S^{(d)}|\alpha\rangle$ get contributions from cases $E_\beta = E_\alpha$ and $E_\beta \neq E_\alpha$, and give $T\Gamma_0$ and $P^{(d)}$ respectively. The deviation of the kinetic energies, $E_\beta - E_\alpha$, in the latter is due to the interaction energy of the overlapping waves, which depends on the coordinate system. Therefore, it is understood that $H_{\rm int}$ is not Lorentz invariant. Thus the kinetic-energy non-conserving term, which was mentioned by Peierls and Landau [4] as giving a negligibly small correction, yields $P^{(d)}$ [5][2]. Because H_0 is a generator of the Poincaré group, Eq. (8) shows that $S^{(d)}[T]$ and $P^{(d)}$ violate the Poincaré invariance. In the system described by Eq. (4), the first term disappears but the second term does not, $\Gamma_0 = 0$, and $P^{(d)} \neq 0$.

$S[T]$ is expressed with the boundary conditions for the scalar field $\phi(x)$ [12,13],

$$\lim_{t\to -T/2}\left\langle\alpha\left|\phi^f\right|\beta\right\rangle = \left\langle\alpha\left|\phi^f_{\rm in}\right|\beta\right\rangle, \tag{10}$$

$$\lim_{t\to +T/2}\left\langle\alpha\left|\phi^f\right|\beta\right\rangle = \left\langle\alpha\left|\phi^f_{\rm out}\right|\beta\right\rangle, \tag{11}$$

where $\phi_{\rm in}(x)$ and $\phi_{\rm out}(x)$ satisfy the free wave equation, and ϕ^f, $\phi^f_{\rm in}$, and $\phi^f_{\rm out}$ are the expansion coefficients of $\phi(x)$, $\phi_{\rm in}(x)$, and $\phi_{\rm out}(x)$, with the normalized wavefunctions $f(x)$ of the form

$$\phi^f(t) = i\int d\vec{x}\, f^*(\vec{x},t)\overleftrightarrow{\partial_0}\phi(\vec{x},t). \tag{12}$$

[2] The unusual enhancement observed in the laser Compton experiment [11] may be connected.

The function $f(x)$ indicates the wavefunction with which the outgoing wave interacts in a successive reaction of the process. The outgoing photon studied in the following section interacts with the atom or nucleus and their wavefunctions are used for $f(x)$. Consequently, $S^{(d)}[T]$ depends on $f(x)$, and it is appropriate to write it as $S^{(d)}[T; f]$. Accordingly, the probability of the events is expressed by this normalized wavefunction, called a wavepacket. Wavepackets that satisfy free wave equations and that are localized in space are important for rigorously defining the scattering amplitude [12,13]. $S^{(d)}[T; f]$ expresses the wave nature due to the states of continuous kinetic energy. $S^{(d)}[T; f]$ does not preserve the Poincaré invariance defined by L_0. The state $|\beta\rangle$ of E_β is orthogonal to $|\alpha\rangle$ of $E_\alpha \neq E_\beta$ and $P^{(d)}$ approaches constant at $T = \infty$.

The wavepackets [8–10,12,13] can be replaced with plane waves for a practical computation of $S[\infty]$ [18–26], but this cannot be done for $P^{(d)}$ [14–16]. $P^{(d)}$ is derived from $S^{(d)}[T; f]$, and depends on $f(x)$.

The photon is massless in vacuum and has a small effective mass determined by the plasma frequency in matter; the neutrino is nearly massless. Thus they have a large wave zone of revealing wave phenomena caused by $P^{(d)}$. These small masses make $P^{(d)}$ appear on a macroscopic scale and significantly affect the physical reactions. In this small (or zero) mass region, the effects of the diffractive term $P^{(d)}$ are pronounced. This is our interest in the present paper. The produced photon interacts with matter with the electromagnetic interaction, which leads to macroscopic observables. The term $P^{(d)}$ of the processes of $\Gamma_0 = 0$, such as 2γ decays of a 1^+ meson and γ and ν reactions, are shown to be relevant to many physical processes, including the possible experimental observation of the relic neutrino. The enhancement of the probability for light particles with intense photons based on the normal component Γ_0 was proposed in Refs. [28,29], and the collective interaction between electrons and the neutrino derived from the normal component Γ_0 was considered in Refs. [30,31]. Our theory is based on the probability $P^{(d)}$ and hence differs from the previous ones in many respects.

This paper is organized in the following manner. In Sect. 2, the coupling of two photons with 1^+ states through a triangle diagram is obtained. In Sects. 3 and 4, positronium and heavy quarkonium are studied and their $P^{(d)}$ are computed. Based on these studies, we go on to investigate the interaction of photons and neutrinos. In Sect. 5, a neutrino–photon interaction of the order of αG_F and various implications for high-energy neutrino phenomena are presented. In Sect. 6, we explore the implication of the photon–neutrino coupling on experimental settings. A summary is given in Sect. 7.

2. Coupling of the 1^+ meson with two photons

The coupling of $\gamma\gamma$ with axial vector states, the 1^+ meson composed of e^-e^+, $q\bar{q}$, and $\nu\bar{\nu}$ are studied using an effective Lagrangian expressed by local fields. From symmetry considerations, an effective interaction of the 1^+ state ϕ_1^μ with two photons has the form

$$S_{\rm int} = g \int d^4x \partial_\mu \left(\phi_1^\mu(x) \tilde{F}_{\alpha\beta}(x) F^{\alpha\beta}(x) \right), \tag{13}$$

$$\partial_\mu \phi_1^\mu(x) = 0, \quad \tilde{F}_{\alpha\beta}(x) = \epsilon_{\alpha\beta\gamma\nu} F^{\gamma\nu}(x),$$

where $F_{\alpha\beta}$ is the electromagnetic field, and the coupling strength g is computed later. In a transition of plane waves in an infinite-time interval, the space-time boundary is at infinity and the transition

amplitude is computed with the plane waves, in the form

$$\mathcal{M} = (p_i - p_f)_\mu (2\pi)^4 \delta^{(4)}(p_i - p_f)\tilde{\mathcal{M}}^\mu, \tag{14}$$

and vanishes, where p_i and p_f are 4D momenta of the initial and final states and $\tilde{\mathcal{M}}^\mu$ is the invariant amplitude. This shows that the amplitude proportional to $\delta^{(4)}(p_i - p_f)$ and the transition rate Γ_0 vanish. The rate of $1^+ \to \gamma\gamma$ decay vanishes in general systems, because the state of two photons of momenta $(\vec{p}, -\vec{p}\,)$ does not couple with a massive 1^+ particle. Hence

$$\Gamma_0^{1^+ \to \gamma\gamma} = 0, \tag{15}$$

which is known as the Landau–Yang theorem [32,33].

The term $S_{\rm int}$ is written as a surface term in 4D space-time,

$$S_{\rm int} = g \int_{\rm surface} dS_\mu \left(\phi_1^\mu(x) \tilde{F}_{\alpha\beta}(x) F^{\alpha\beta}(x) \right), \tag{16}$$

which is determined by the wavefunctions of the initial and final states. Accordingly, the transition amplitude derived from this surface action is not proportional to T, but has a weaker T dependence. Thus $P^{(d)}$ comes from the surface term, and does not have the delta function of kinetic-energy conservation. The kinetic energy of the final states deviates from that of the initial state due to the finite interaction energy between them. The deviation becomes larger and $P^{(d)}$ is expected to increase with a larger overlap. We find $P^{(d)}$ in the following.

2.1. Triangle diagram

The interaction of the form Eq. (13) is generated by the one-loop effect in the standard model. In QED, we have

$$\begin{aligned} L &= L_0 + L_{\rm int}, \quad L_0 = \bar{l}(x)(\gamma \cdot p - m_l) l(x) - \tfrac{1}{4} F_{\mu\nu}(x) F^{\mu\nu}(x), \\ L_{\rm int} &= e J_\mu A^\mu(x), \quad J_\mu(x) = \bar{l}(x)\gamma_\mu l(x), \end{aligned} \tag{17}$$

where $A^\mu(x)$ is the photon field and $l(x)$ is the electron field. The scalar and axial vector currents

$$J(0) = \bar{l}(0) l(0), \tag{18}$$

$$J^{5,\mu} = \bar{l}(0)\gamma_5\gamma^\mu l(0) \tag{19}$$

couple with two photons in the bulk through the triangle diagram, Fig. 1. The matrix elements are

$$\Gamma_0 = \langle 0|J(0)|k_1, k_2\rangle = \frac{e^2}{4\pi^2} \epsilon^\mu(k_1)\epsilon^\nu(k_2) m[(k_2)_\mu (k_1)_\nu - g_{\mu\nu} k_1 \cdot k_2] f_0, \tag{20}$$

$$\begin{aligned} \Gamma_{5,\alpha} = \langle 0|J_{5,\alpha}(0)|k_1, k_2\rangle &= -i \frac{e^2}{4\pi^2} 2 f_1 \epsilon^{\mu_1}(k_1)\epsilon^{\mu_2}(k_2) \\ &\times \left[((k_1)_{\mu_2} \epsilon_{\mu_1\nu_1\nu_2\alpha} - (k_2)_{\mu_1} \epsilon_{\mu_2\nu_1\nu_2\alpha}) k_1^{\nu_1} k_2^{\nu_2} + (k_1 \cdot k_2) \epsilon_{\mu_1\mu_2\nu\alpha} (k_1 - k_2)^\nu \right], \end{aligned} \tag{21}$$

where $\epsilon_\mu(\vec{k})$ is the polarization vector for the photon. The triangle diagram for the axial vector current, Eq. (21), has been studied in connection with axial anomaly and $\pi^0 \to \gamma\gamma$ decay [34–38] and

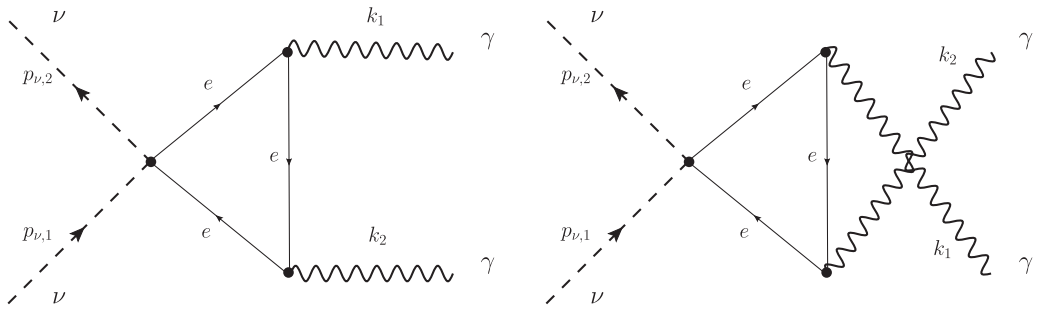

Fig. 1. Triangle diagrams of the electron loop that give contributions to $1^+(l\bar{l}) \to \gamma\gamma$, $\nu + \gamma \to \nu + \gamma$, and $\nu + \bar{\nu} \to \gamma + \gamma$.

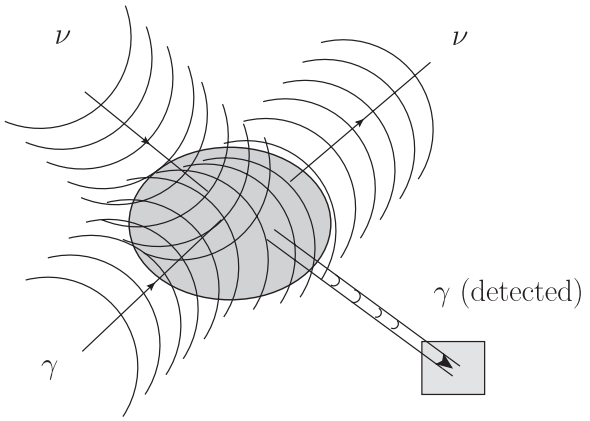

Fig. 2. Diagram of the neutrino–photon scattering, $\nu + \gamma \to \nu + \gamma$, of spatially spread waves.

is now applied to $P^{(d)}$ for two-photon transitions of the axial vector meson and neutrino. The triangle diagram, Fig. 1, shows that the interaction occurs locally in space and time, but the transition amplitude is the integral over the coordinates and receives a large diffractive contribution if the neutrino and photon are spatially spread waves. In Fig. 1, the incoming and outgoing waves are expressed by lines, but they are in fact spread waves, which is obvious in the figures in Ref. [39] and in Fig. 2.

$\Gamma_{5,\alpha}$ is expressed also with f_1 in the form

$$\Gamma_{5,\alpha} = \frac{\alpha_{\rm em}}{2\pi} f_1 (k_1 + k_2)_\alpha \left(\tilde{F}_{1,\rho\lambda} F_2^{\rho\lambda} + \tilde{F}_{2,\rho\lambda} F_1^{\rho\lambda} \right), \tag{22}$$

$$F_{1,\rho\lambda} = k_{1,\rho}\epsilon_{1,\lambda} - k_{1,\lambda}\epsilon_{2,\rho},\ \tilde{F}_{\rho\lambda} = \frac{1}{2}\epsilon_{\rho\lambda\xi\eta}F^{\xi\eta}.$$

The coefficients f_0 and f_1 are given by the integral over the Feynman parameters,

$$f_0 = \int_0^1 dx \int_0^{1-x} dy \frac{1}{m_l^2 - 2xyk_1 \cdot k_2 - i\epsilon}, \tag{23}$$

$$f_1 = \int_0^1 dx \int_0^{1-x} dy \frac{xy}{m_l^2 - 2xyk_1 \cdot k_2 - i\epsilon}, \tag{24}$$

where

$$f_1 = -\frac{1}{4k_1\cdot k_2} + \frac{m_l^2}{4(k_1\cdot k_2)^2} I_1, \tag{25}$$

$$\begin{aligned} I_1 &= 2k_1\cdot k_2 \int_0^1 dx \int_0^{1-x} dy \frac{1}{m_l^2 - 2xyk_1\cdot k_2 - i\epsilon} \\ &= \begin{cases} 2\mathrm{Sin}^{-1}\left(\sqrt{\frac{k_1\cdot k_2}{2m_l^2}}\right), & \text{if } k_1\cdot k_2 < 2m_l^2, \\ \frac{\pi^2}{2} - \frac{1}{2}\log^2 \frac{1+\sqrt{1-\frac{2m_l^2}{k_1\cdot k_2}}}{1-\sqrt{1-\frac{2m_l^2}{k_1\cdot k_2}}} + i\pi \log \frac{1+\sqrt{1-\frac{2m_l^2}{k_1\cdot k_2}}}{1-\sqrt{1-\frac{2m_l^2}{k_1\cdot k_2}}}, & \text{if } k_1\cdot k_2 \geq 2m_l^2. \end{cases} \end{aligned} \tag{26}$$

f_1 in various kinematical regions is

$$f_1 = \begin{cases} \dfrac{-1}{4k_1\cdot k_2} + \dfrac{m^2}{4(k_1\cdot k_2)^2}\pi\left(1 - \dfrac{2\delta E}{m_l}\right); & k_1\cdot k_2 = 2m_l^2 - m_l\delta E, \\ \dfrac{-1}{4k_1\cdot k_2}; & k_1\cdot k_2 \gg m_l^2, \\ \dfrac{1}{2m_l^2}; & k_1\cdot k_2 \ll m_l^2. \end{cases} \tag{27}$$

3. Positronium

The bound states of e^+e^- with the orbital angular momentum $L = 1$, $S = 1$ have total angular momentum $J = 2, 1, 0$. These states at rest of $\vec{P} = 0$ are expressed with non-relativistic wavefunctions and creation operators of e^+ and e^- of momentum $\vec{p}$, spin $\pm 1/2$, and P-wave wavefunctions $p_i F(p)$ as given in Appendix A, where

$$\left|\frac{1}{2}, \frac{1}{2}; -1\right\rangle = \int d\vec{p}\, b^\dagger_{+\frac{1}{2}}(\vec{p}) d^\dagger_{+\frac{1}{2}}(-\vec{p})(p_x - ip_y)F(p)|0\rangle. \tag{28}$$

Others are defined in the same manner.

These bound states couple with the electron pairs with effective local interactions, which are expressed as

$$L_{\mathrm{int}} = g_0\phi_0(x)\bar{e}(x)e(x) + g_1\phi_1^\mu(x)\bar{e}(x)\gamma^5\gamma_\mu e(x) + g_2\phi_2^{\mu\nu}(x)\bar{e}(x)\gamma_\mu\partial_\nu e(x), \tag{29}$$

where the coupling strengths are computed from

$$g_0 = \left\langle 0|\bar{e}(0)e(0)|\phi_0;\, \vec{P} = 0\right\rangle, \tag{30}$$

$$g_1\epsilon^\mu(\vec{P} = 0) = \left\langle 0|\bar{e}(0)\gamma^5\gamma^\mu e(0)|\phi_1;\, \vec{P} = 0\right\rangle, \tag{31}$$

$$g_2\epsilon^{\mu\nu}(\vec{P} = 0) = \left\langle 0|\bar{e}(0)\gamma^\mu\partial^\nu e(0)|\phi_2;\, \vec{P} = 0\right\rangle, \tag{32}$$

where the ϵ^μ, $\epsilon^{\mu\nu}$ are polarization vectors or tensors for the massive vector and tensor mesons. We have

$$\begin{aligned} g_0 = gN_0, \quad g_1 = gN_1, \quad g_2 = gN_2, \\ g = -2\pi \int dp\, p^4 F(p) \frac{2}{|E| + M}, \\ N_0 = 1, \quad N_1 = 0.862, \quad N_2 = 1.33. \end{aligned} \tag{33}$$

The decay rates for 0^+ and 2^+ were studied in Refs. [40,41], so that here we concentrate on 1^+ and 0^+ as a reference for 1^+.

Fields $\phi_0(x)$, $\phi_1(x)$, and $\phi_2(x)$ couple with two photons through the triangle diagrams. Their interactions with two photons are summarized in the following effective Lagrangian:

$$L_{\rm int} = g_0 \frac{\alpha}{\pi} f_0 \phi_0 F_{\mu\nu} F^{\mu\nu} + g_1 \frac{\alpha}{\pi} \partial_\mu \left(f_1 \phi_1^\mu \epsilon_{\nu\rho\sigma\tau} F^{\nu\rho} F^{\sigma\tau} \right) + g_2 \frac{\alpha}{\pi} T^{\mu\nu} F_{\mu\rho} F^{\rho\nu}. \tag{34}$$

3.1. *Axial vector positronium*

Here we study the two-photon decay of axial vector positronium, which is governed by the second term on the right-hand side of Eq. (34). The matrix element of the axial current between the vacuum and two-photon state was computed by Refs. [34–38]. Because the Γ_0 of two-photon decay of the axial vector meson vanishes due to the Landau–Yang theorem, but $P^{(d)}$ does not, we give the detailed derivation of $P^{(d)}$.

From the effective interaction, Eq. (34), the probability amplitude of the event that one of the photons of $\vec{k}_\gamma$ from the decay of c_μ of $\vec{p}_c$ is detected at $(\vec{X}_\gamma, T_\gamma)$ is

$$\mathcal{M} = -g_1 \frac{\alpha}{\pi} \int d^4x \frac{\partial}{\partial x_\mu} \left[f_1 \langle 0 | c_\mu(x) | \vec{p}_c \rangle \langle (\vec{k}_\gamma, \vec{X}_\gamma, T_\gamma), k_1 | \epsilon_{\nu\rho\sigma\tau} F^{\nu\rho} F^{\sigma\tau} | 0 \rangle \right], \tag{35}$$

where

$$\begin{aligned}
\left\langle \vec{k}_\gamma, \vec{X}_\gamma, T_\gamma | A^\mu(x) | 0 \right\rangle &= N_\gamma \int d\vec{k}_2 \rho_\gamma(\vec{k}_2) e^{-\frac{\sigma_\gamma}{2}(\vec{k}_2 - \vec{k}_\gamma)^2 + i(E(\vec{k}_2)(t - T_\gamma) - \vec{k}_2 \cdot (\vec{x} - \vec{X}_\gamma))} \epsilon^\mu(\vec{k}_2), \\
\left\langle \vec{k}_1 | A^\mu(x) | 0 \right\rangle &= \rho_\gamma(\vec{k}_1) \epsilon^\mu(\vec{k}_2) e^{i(E(\vec{k}_1)t - \vec{k}_1 \cdot \vec{x})}, \\
\left\langle 0 | c_\mu(x) | \vec{p}_c \right\rangle &= (2\pi)^{\frac{3}{2}} \rho_c(\vec{p}_c) \epsilon_\mu(\vec{p}_c) e^{-i(E(\vec{p}_c)t - \vec{p}_c \cdot \vec{x})}.
\end{aligned} \tag{36}$$

The initial state is normalized, and the coupling in Eq. (33) has $(2\pi)^{\frac{3}{2}}$ for the initial state, and

$$\begin{aligned}
k_\mu \epsilon^\mu(k) = 0, \quad (p_c)_\mu \epsilon^\mu(p_c) = 0, \\
\rho_i(\vec{k}) = \left(\frac{1}{2E_i(\vec{k})(2\pi)^3} \right)^{\frac{1}{2}}, \quad i = c \text{ or } \gamma.
\end{aligned} \tag{37}$$

The state $\langle \vec{k}_\gamma, \vec{X}_\gamma, T_\gamma |$ is normalized, and

$$N_\gamma = \left(\frac{\sigma_\gamma}{\pi} \right)^{\frac{3}{4}}. \tag{38}$$

Integration over $\vec{k}_2$ is made prior to the integration over x, in order for $\mathcal{M}$ to satisfy the boundary condition of $S[T]$, and we have

$$\begin{aligned}
\left\langle \vec{k}_\gamma, \vec{X}_\gamma, T_\gamma \left| A^\mu(x) \right| 0 \right\rangle = \theta(\lambda) \left(\frac{(2\pi)^3}{\sigma_\gamma \sigma_T^2} \right)^{\frac{1}{2}} \rho_\gamma \left(\vec{k}_\gamma + \delta\vec{k} \right) \epsilon^\mu \left(\vec{k}_\gamma + \delta\vec{k} \right) \\
\times e^{i\left(E\left(\vec{k}_\gamma\right)(t - T_\gamma) - \vec{k}_\gamma \cdot \left(\vec{x} - \vec{X}_\gamma \right) \right) - \chi(x)},
\end{aligned} \tag{39}$$

where

$$\lambda = (t - T_\gamma)^2 - \left(\vec{x} - \vec{X}_\gamma\right)^2, \tag{40}$$

$$\chi(x) = \frac{1}{2\sigma_\gamma}\left(\left(\vec{x} - \vec{X}_\gamma\right)_l - v_\gamma(x_0 - T_\gamma)\right)^2 + \frac{1}{2\sigma_T}\left(\vec{x} - \vec{X}_\gamma\right)_T^2, \tag{41}$$

$$\left(\delta\vec{k}(x)\right)_i = -\frac{i}{\sigma_\gamma^i}\delta\vec{x}, \quad \delta\vec{x} = \left(\vec{x} - \vec{X}_\gamma - \vec{v}_\gamma(t - T_\gamma)\right),$$

$$\sigma_\gamma^l = \sigma_\gamma; \quad i = \text{longitudinal}, \quad \sigma_\gamma^T = \sigma_T; \quad i = \text{transverse}.$$

The wavepacket expands in the transverse direction, and σ_T in large $x_0 - T_\gamma$ is given by

$$\sigma_T = \sigma_\gamma - \frac{i}{E_\gamma}(x_0 - T_\gamma). \tag{42}$$

We later use

$$\sum_{\text{spin}} \epsilon_\mu\left(\vec{k}_\gamma + \delta\vec{k}\right)\epsilon_\nu\left(\vec{k}_\gamma + \delta\vec{k}\right) = -g_{\mu\nu}, \tag{43}$$

$$\delta k^0(x) = \frac{i}{\sigma_\gamma}\delta x^0, \quad \delta x^0 = \vec{v}\cdot\left(\vec{x} - \vec{X}_\gamma - \vec{v}_\gamma(t - T_\gamma)\right).$$

The stationary phase for large $x_0 - T_\gamma$ exists in the time-like region $\lambda \geq 0$ [14], and the function in Eq. (39) and its derivative are proportional to $\theta(\lambda)$. Thus the integration in Eq. (35) is made over the region $\lambda \geq 0$, which has the boundary $\lambda = 0$. Consequently, the transition amplitude does not vanish if the integrand at the boundary is finite. It is shown that this is, in fact, the case. σ_γ is the size of the nucleus or atomic wavefunction with which the photon interacts and is estimated later. For the sake of simplicity, we use the Gaussian form for the main part of this paper.

Substituting Eq. (21), we have the amplitude

$$\mathcal{M} = -ig_1\frac{\alpha}{\pi}N\int_{\lambda\geq 0} d^4x\frac{\partial}{\partial x^\mu}\left[e^{i(p_c - k_1)\cdot x}\tilde{\mathcal{M}}^\mu\right], \tag{44}$$

$$\tilde{\mathcal{M}}^\mu = f_1\left(k_1\cdot(k_\gamma + \delta k(x))\right)e^{i(E(k_\gamma)(t - T_\gamma) - \vec{k}_\gamma\cdot(\vec{x} - \vec{X}_\gamma)) - \chi(x)}T^\mu,$$

$$T^\mu = \epsilon^\mu(p_c)\epsilon^\nu(k_1)^*\epsilon_{\rho\lambda\xi\nu}k_1^\xi(k_\gamma + \delta k_\gamma(x))^\rho\epsilon^\lambda(k_\gamma + \delta k_\gamma(x)),$$

$$N = (2\pi)^{\frac{3}{2}}\rho_c(\vec{p}_c)\rho_\gamma(\vec{k}_\gamma)\rho_\gamma(\vec{k}_1)N_\gamma\left(\frac{(2\pi)^3}{\sigma_\gamma\sigma_T^2}\right)^{\frac{1}{2}}, \tag{45}$$

which depends on the momenta and coordinates $(T_\gamma, \vec{X}_\gamma)$ of the final state and the time of the initial state T_m. Although $\mathcal{M}$ is written as the integral over the surface, $\lambda = 0$, Eq. (44) is useful and is applied for computing the probability per particle:

$$P = \frac{1}{V}\int\frac{d\vec{X}_\gamma}{(2\pi)^3}d\vec{k}_\gamma d\vec{k}_1\sum_{\text{spin}}|\mathcal{M}|^2, \tag{46}$$

where V is a normalization volume for the initial state, the momentum of the non-observed final state is integrated over the whole positive energy region, and the position of the observed particle is integrated inside the detector.

Following the method of the previous works [1,2] and Appendix B, we write the probability with a correlation function. In the integral

$$\int d\vec{k}_1 |\mathcal{M}|^2 = \left(\frac{g\alpha N}{\pi}\right)^2 \int d\vec{k}_1 \rho_\gamma^2(\vec{k}_1) \int_{\lambda_1,\lambda_2\geq 0} d^4x_1 d^4x_2 \frac{\partial^2}{\partial_1^{\mu_1}\partial_2^{\mu_2}} F, \tag{47}$$

$$F = f_1\left(k_1\cdot(k_\gamma+\delta k_\gamma(x_1))\right) f_1^*\left(k_1\cdot(k_\gamma+\delta k_\gamma(x_2))\right) T^{\mu_1}(x_1)\left(T^{\mu_2}(x_2)\right)^* \times e^{-i(p_c-k_1-k_\gamma)\cdot(x_1-x_2)-\chi(x_1)-\chi^*(x_2)},$$

we have

$$\sum_{\text{spin}} T^{\mu_1}(x_1)\left(T^{\mu_2}(x_2)\right)^* = 2(-g^{\mu_1\mu_2}+p_c^{\mu_1}p_c^{\mu_2}/M^2)(k_1\cdot(k_\gamma+\delta k_\gamma(x_2)^*))(k_1\cdot(k_\gamma+\delta k(x_1))). \tag{48}$$

With variables

$$x_+^\mu = \frac{x_1^\mu + x_2^\mu - 2X^\mu}{2}, \quad X_0 = T_\gamma, \tag{49}$$

$$\delta x^\mu = x_1^\mu - x_2^\mu, \tag{50}$$

the integral is written as

$$\int_{\lambda_i\geq 0} d^4x_1 d^4x_2 \frac{\partial^2}{\partial x_1^\mu \partial x_{2,\mu}} F = \int_{\lambda_+\geq 0} d^4x_+ d^4\delta x \left(\frac{1}{4}\frac{\partial^2}{\partial {x_{+,\mu}}^2} - \frac{\partial^2}{\partial \delta {x_\mu}^2}\right) F \tag{51}$$

$$= \int d^4\delta x \int_{\lambda_+=0} \frac{1}{4} d^3 S_+^\mu \frac{\partial}{\partial x_{+,\mu}} F, \tag{52}$$

where $\lambda_+ = x_+^2$, x_+ is integrated over the region $\lambda_+ \geq 0$, and the integral is computed with the value at the boundary, $\lambda_+ = 0$. δx are integrated over the whole region, and the second term in the second line vanishes.

Using the formulae [1,2]

$$\frac{1}{(2\pi)^3}\int \frac{d\vec{k}_1}{2E(k_1)} e^{-i(p_c-k_1)\cdot\delta x} = -i\frac{\epsilon(\delta t)}{4\pi}\delta(\lambda_-)\theta(\text{phase space}) + \text{regular},$$

$$\theta(\text{phase space}) = \theta(M^2 - 2p_c\cdot p_\gamma), \tag{53}$$

$$\int d\delta\vec{x} e^{ip_\gamma\cdot\delta\vec{x} - \frac{1}{4\sigma}(\delta\vec{x}-\vec{v}\delta t)^2} \frac{1}{4\pi}\delta(\lambda) = \frac{\sigma_T}{2}\frac{e^{i\bar{\phi}_c(\delta t)}}{\delta t}, \tag{54}$$

$$\bar{\phi}_c(\delta t) = \omega_\gamma \delta t, \quad \omega_\gamma = \frac{m_\gamma^2}{2E_\gamma},$$

and the integrals given in Appendix E, we compute the probability. It is worthwhile to note that the light-cone singularity exists in the kinematical region θ(phase space) and the probability becomes finite in this region [1,2]. Natural units, $c = \hbar = 1$, are used in the majority of places, but c and $\hbar$ are

written explicitly when it is necessary, and SI units are used in later parts. After tedious calculations, we have the probability

$$P = \frac{1}{3}\int \frac{d\vec{X}_\gamma}{V}\frac{d\vec{p}_\gamma}{(2\pi)^3 E_\gamma} N_2 \frac{1}{4\pi}\left(i\sum_i I_i\right)\Delta_{1^+,\gamma}\theta(M^2 - 2p_c\cdot p_\gamma), \tag{55}$$

where I_i is given in Appendix E, and

$$N_2 = \left(g\frac{2}{\pi}\alpha\right)^2 \frac{1}{2E_c}\left(\frac{\pi}{\sigma_\gamma}\right)^{\frac{3}{2}}, \tag{56}$$

$$\Delta_{1^+,\gamma} = \left|f_1((p_c - k_\gamma)\cdot k_\gamma)\right|^2 2((p_c - k_\gamma)\cdot k_\gamma)^2 = \frac{(\pi-2)^2}{32};\ (\delta E \to 0), \tag{57}$$

and

$$\left(\frac{\pi^3\sigma_\gamma}{\sigma_T^2(x_1)(\sigma_T^*(x_2))^2}\right)^{\frac{1}{2}} = \left(\frac{\pi^3}{\sigma_\gamma^3}\right)^{\frac{1}{2}}\rho_s\left(x_1^0 - x_2^0\right), \tag{58}$$

$$\rho_s(x_1^0 - x_2^0) = 1 + i\frac{x_1^0 - x_2^0}{E_\gamma\sigma_\gamma}$$

were substituted.

Integrating over the gamma's coordinate $\vec{X}_\gamma$, we obtain the total volume, which is canceled by the factor V^{-1} from the normalization of the initial state. The total probability, for the high-energy gamma rays, is then expressed as

$$P = \frac{1}{3}\pi^2\left\{\sigma_l^2\log(\omega_\gamma T) + \frac{\sigma_\gamma}{m_\gamma^2}\right\}\int\frac{d\vec{p}_\gamma}{(2\pi)^3 E_\gamma}\frac{1}{2}N_2\theta\left(M^2 - 2p_c\cdot p_\gamma\right)\Delta_{1^+,\gamma}, \tag{59}$$

where $\mathrm{L} = cT$ is the length of the decay region. The kinematical region of the final states is expressed by the step function [2], which is different from the on-mass shell condition. Γ_0 vanishes and P is composed of $\log T$ and constant terms. The constant is inversely proportional to m_γ^2, and becomes large for small m_γ.

3.2. Transition probability

A photon γ is massless in vacuum and has an effective mass in matter, which is given by plasma frequency in matter [42] as

$$m_{\mathrm{eff}} = \hbar\sqrt{\frac{n_e e^2}{m_e\epsilon_0}} = \hbar\sqrt{\frac{4\pi\alpha n_e\hbar c}{m_e}}, \tag{60}$$

where n_e is the density of the electron, and for the value

$$n_e^0 = \frac{1}{(10^{-10})^3}(\mathrm{m})^{-3} = 10^{30}(\mathrm{m})^{-3}. \tag{61}$$

Substituting

$$\alpha = \frac{1}{137},\ m_e = 0.5\,\mathrm{MeV}/c^2, \tag{62}$$

we have

$$m_{\mathrm{eff}}c^2 = 30\sqrt{\frac{n_e}{n_e^0}}\,\mathrm{eV}. \tag{63}$$

In the air, $n_e = 3 \times 10^{25}/\mathrm{m}^3$, the mass agrees with

$$m_{\mathrm{eff}}c^2 = 4 \times 10^{-3}\,\mathrm{eV}, \tag{64}$$

which is comparable to the neutrino mass. At a macroscopic T,

$$\omega_\gamma T = \frac{T}{T_0},\ T_0^{-1} = \frac{m_{\mathrm{eff}}^2 c^4}{\hbar E_\gamma} = 900\frac{n_e}{n_e^0}\frac{1}{6\times 10^{-16}\times 10^6}\,\mathrm{s}^{-1}, \tag{65}$$

$\omega_\gamma T$ is much larger than 1.

We have the probability at the system of $p_c = (E_c, 0, 0, p_c)$,

$$\frac{dP}{dp_\gamma} = C\left(\left(1-\frac{E_c}{p_c}\right)p_\gamma + \frac{M^2}{2p_c}\right);\quad \frac{M^2}{2(E_c+p_c)} \le p_\gamma \le \frac{M^2}{2(E_c-p_c)}, \tag{66}$$
$$C = \frac{\pi^2}{3}\left(3\sigma_\gamma^2 \log\frac{T}{T_0} + \frac{1}{4}\frac{\sigma_\gamma}{m_\gamma^2}\right)\frac{N_2}{2}\Delta_{1^+,\gamma},$$

and the total probability

$$P_{\mathrm{total}} = \frac{(\pi-2)^2}{1536}\frac{1}{\sqrt{\pi}}\left(3\sqrt{\sigma}_\gamma \log\frac{T}{T_0} + \frac{1}{4}\frac{1}{m_\gamma^2\sqrt{\sigma}_\gamma}\right)(g\alpha)^2\frac{E_c+2p_c}{E_c(E_c+p_c)}. \tag{67}$$

4. Heavy quarkonium

The decay of axial vector mesons composed of heavy quarks exhibits the same phenomena. Heavy quark mesons composed of charm and bottom quarks are observed, and show rich decay properties in the two-photon decay, radiative transitions, and two-gluon decays. Because quarks interact via electromagnetic and strong interactions, non-perturbative effects are not negligible, but the symmetry consideration is valid. Moreover, the non-relativistic representations are good for these bound states, because quark masses are much greater than the confinement scale. Furthermore, they have small spatial sizes. Accordingly, we represent them with local fields and find their interactions using the coupling strengths of Eq. (33) and the values of the triangle diagrams, Eqs. (20) and (21).

4.1. $q\bar{q} \to \gamma + \gamma$

Up and down quarks have charge $2e/3$ or $e/3$, and color triplet. Hence the probabilities of two-photon decays are obtained by Eq. (67) with charges of quarks $2e/3$, $e/3$, and color factor. It is highly desirable to obtain the experimental value for 1^+.

4.2. $q\bar{q} \to$ gluon + gluon

A meson composed of heavy quarks decays to light hadrons through gluons. Color singlet two-gluon states are equivalent to two-photon states. Accordingly, the two-gluon decays are calculated in the equivalent way to that of two-photon decays as far as the perturbative calculations are concerned. The transition rates for 0^+ and 2^+ may be calculated in this manner. The total rates for $L = 0$ charmonium, J/Ψ and η_c, agree with the values obtained by the perturbative calculations. J/Ψ is $C = -1$ and decays to three gluons and the latter is $C = +1$ and decays to two gluons. The former rate is of α_s^3 and the latter rate is of α_s^2, where α_s is the coupling strength of the gluon. Their widths are $\Gamma = 93\,\mathrm{keV}$ or $\Gamma = 26.7\,\mathrm{MeV}$, and are consistent with the small coupling strength $\alpha_s \approx 0.2$. Now $L = 1$ states have $C = +1$. Hence a meson of $J = 2$ and that of $J = 0$ decay to two gluons, whereas the decay rate of a $J = 1$ meson vanishes by the Landau–Yang theorem.

A $c\bar{c}$ meson of the quantum number 1^+ is slightly different from that of positronium, because a gluon hadronizes by a non-perturbative effect, which is peculiar to the gluon. The hadronization length is not rigorously known, but it would be reasonable to assume that the length is on the order of the size of the pion. The time interval T is then a microscopic value. $P^{(d)}$ for this time T is estimated in the following.

A gluon also hadronizes in the interval of the lightest hadron size:

$$T = \frac{R_{\rm hadron}}{c} = \frac{c\hbar}{m_\pi}. \tag{68}$$

The gluon plasma frequency is estimated from the quark density,

$$m_{\rm eff} = \sqrt{\frac{n_q e^2_{\rm strong}}{m_q \epsilon_0}}, \tag{69}$$

and

$$n_q = \frac{1}{({\rm fm})^3}, \quad \alpha_s = 0.2, \quad m_q c^2 = 2\,{\rm MeV}. \tag{70}$$

Then we have

$$\begin{aligned}\omega_g T &= \frac{m^2_{\rm eff} c^4 T}{E_g} = \frac{c^4 \alpha_s^2}{({\rm fm})^3 m_q m_\pi E_g} = \frac{(c\hbar)^3}{m_q m_\pi E_g ({\rm fm})^3}\alpha_s^2 \\ &= \frac{(197\,{\rm MeV})^3}{2 \times 130 \times 1500\,({\rm MeV})^3} \times 4 \times 10^{-2} = 0.9.\end{aligned} \tag{71}$$

At small $\omega_g T$, $\tilde{g}(\omega_g T)$ varies with T, as shown in Fig. 2 of Ref. [2] and

$$\tilde{g}(\omega_g T)|_{\omega_g T = 1} = 2.5. \tag{72}$$

Higher-order corrections also modify the rates for $q\bar{q}$. The values to light hadrons are estimated by Refs. [43–47]. The total values for light hadrons are expressed with singlet and octet components H_1 and H_8 as

$$\Gamma(\chi_0 \to \text{light hadrons}) = 6.6\alpha_s^2 H_1 + 3.96 H_8 \alpha_s^2, \tag{73}$$

$$\Gamma(\chi_1 \to \text{light hadrons}) = 0 \times \alpha_s^2 H_1 + 3.96 H_8 \alpha_s^2, \tag{74}$$

$$\Gamma(\chi_2 \to \text{light hadrons}) = 0.682\alpha_s^2 H_1 + 3.96 H_8 \alpha_s^2. \tag{75}$$

Using values for χ_0 and χ_2 from Ref. [51],

$$\Gamma(\chi_0 \to \text{light hadrons}) = 1.8\,{\rm MeV}, \tag{76}$$

$$\Gamma(\chi_2 \to \text{light hadrons}) = 0.278\,{\rm MeV}, \tag{77}$$

we have the rate for χ_1 from H_8,

$$\Gamma^{(8)}(\chi_1 \to \text{light hadrons}) = 0.056\,{\rm MeV}. \tag{78}$$

The experimental value for χ_1 is

$$\Gamma(\chi_1 \to \text{light hadrons}) = 0.086\,{\rm MeV}\ \text{(world average)}, \tag{79}$$

$$\Gamma(\chi_1 \to \text{light hadrons}) = 0.139\,{\rm MeV}\ \text{(BESS II)}. \tag{80}$$

The large discrepancy among experiments for $\Gamma_{\chi_1 \to \text{light hadrons}}$ may suggest that the value depends on the experimental situation, which may be a feature of $P^{(d)}$. We have

$$\Delta\Gamma = \Gamma(\chi_1 \to \text{light hadrons}) - \Gamma^{(8)}(\chi_1 \to \text{light hadrons}), \tag{81}$$

$$\Delta\Gamma(\text{world average}) = 0.030\,\text{MeV}, \tag{82}$$

$$\Delta\Gamma(\text{BESSII}) = 0.083\,\text{MeV},$$

which are attributed to $P^{(d)}$.

4.3. *E1 transition:* $\Psi' \to \phi_1 + \gamma,\ \phi_1 \to J/\Psi + \gamma$

ϕ_1 is produced in the radiative decays of Ψ' through the E_1 transition

$$\Psi' \to \phi_1 + \gamma, \tag{83}$$

which is expressed by the effective interaction

$$S_{\text{int}} = e' \int d^4x\, O^{\mu\nu} F_{\mu\nu}, \quad O^{\mu\nu} = \epsilon^{\mu\nu\rho\sigma} \Psi'_\mu \phi_{1,\nu} \tag{84}$$

in the local limit. The action Eq. (84) does not take the form of the total derivative, but is written as

$$S_{\text{int}} = e' \int d^4x\, \partial_\nu (O^{\mu\nu} A_\mu) - e' \int d^4x (\partial_\nu O^{\mu\nu}) A_\mu. \tag{85}$$

The second term shows the interaction of the local electromagnetic coupling of the current $j^\mu = \partial_\nu O^{\mu\nu}$ and the first term shows the surface term. This leads to the constant probability at a finite T, $P^{(d)}$. The induced $P^{(d)}$ for muon decay was computed in Ref. [1], and the continuous energy spectrum and large total probability from $P^{(d)}$ compared with $T\Gamma_0$ was found in the region $cT = 1\,\text{m}$.

The radiative transitions of heavy quarkonium are deeply connected with other radiative transitions and a detailed analysis will be presented elsewhere.

Spin 0 and 2 mesons, ϕ_0 and ϕ_2, show the same E_1 transitions and photons show the same behavior from $P^{(d)}$ [48–51]. A pair of photons of the continuous energy spectrum are produced in the wave zone, and are correlated. On the other hand, a pair of photons of the discrete energy spectrum are produced in the particle zone and are not correlated. Thus the photons in the continuous spectrum are different from the simple background, and it would be possible to confirm the correlation by measuring the time coincidence of the two photons.

5. Neutrino–photon interaction

The neutrino–photon interaction of the strength αG_F induced from higher-order effects vanishes due to the Landau–Yang–Gell-Mann theorem. But $P^{(d)}$ is free from the theorem and gives observable effects. Moreover, although the strength seems much weaker than the normal weak-interaction process, it is enhanced drastically if the photon's effective mass is extremely small. Because $P^{(d)}$ does not preserve Lorentz invariance, a careful treatment is required. The triangle diagram of Fig. 1 is expressed in terms of the action

$$S_{\nu\gamma} = \frac{1}{2\pi}\alpha\frac{G_F}{\sqrt{2}} \int d^4x \frac{\partial}{\partial x_\mu} \left(f_1 J^A_\mu(x) \tilde{F}_{\alpha\beta} F^{\alpha\beta} \right), \tag{86}$$

$$J^A_\mu(x) = \bar{\nu}(x)(1-\gamma_5)\gamma_\mu \nu(x),$$

where the axial vector meson in Eq. (34) was replaced by the neutrino current. The mass of the neutrino is extremely small, and was neglected. The $S_{\nu\gamma}$ leads to the neutrino gamma reactions with $\Gamma_0 = 0$, $P^{(d)} \neq 0$ on the order of αG_F.

5.1. $\nu + \gamma \to \nu + \gamma$

The rates Γ_0 of the events

$$\nu + \bar{\nu} \to \gamma + \gamma, \qquad \nu + \gamma \to \nu + \gamma \tag{87}$$

vanish on the order of αG_F [52] due to the Landau–Yang theorem. The higher-order effects were also shown to be extremely small [36] and these processes have been ignored. The theorem is derived from the rigorous conservation law of the kinetic energy and angular momentum. However, these do not hold in $P^{(d)}$, due to the interaction energy caused by the overlap of the initial and final wavefunctions. Consequently, neither $P^{(d)}$ nor the transition probability vanish. These processes are reconsidered with $P^{(d)}$.

From Eq. (86), we have the probability amplitude of the event in which one of the photons of $\vec{k}_\gamma$ interacts with another object or is detected at $\vec{X}_\gamma$ as

$$\mathcal{M} = -\frac{G_F \alpha}{2\pi\sqrt{2}} \int d^4x \frac{\partial}{\partial x_\mu} \left[f_1 \left\langle p_{\nu,2} \left| J^A_\mu(x) \right| p_{\nu,1} \right\rangle \left\langle \left(\vec{k}_\gamma, \vec{X}_\gamma, T_\gamma \right) \left| \tilde{F}_{\alpha\beta} F^{\alpha\beta} \right| k_1 \right\rangle \right]. \tag{88}$$

The amplitude is expressed in the same manner as Eq. (44),

$$\begin{aligned}
\mathcal{M} &= -i \frac{G_F}{\sqrt{2}} \frac{2}{\pi} \alpha N \int_{\lambda \geq 0} d^4x \frac{\partial}{\partial x^\mu} \left[e^{-i(p_{\nu,1} - p_{\nu,2} + k_1)\cdot x} \tilde{\mathcal{M}}^\mu \right], \\
\tilde{\mathcal{M}}^\mu &= f_1(k_1 \cdot k_\gamma) e^{i(E(k_\gamma)(t - T_\gamma) - \vec{k}_\gamma \cdot (\vec{x} - \vec{X}_\gamma)) - \chi(x)} T^\mu, \\
T^\mu &= \bar{\nu}(p_{\nu,2})(1 - \gamma_5)\gamma^\mu \nu(p_{\nu,1}) \epsilon_{\alpha\beta\xi\zeta} \epsilon^\alpha \left(\vec{k}_1 \right) \epsilon^\beta \left(\vec{k}_\gamma + \delta\vec{k}(x) \right) k_1^\xi \left(k_\gamma + \delta k(x) \right)^\zeta, \\
N &= \left(\frac{(2\pi)^3}{\sigma_\gamma \sigma_T^2} \right)^{\frac{1}{2}} N_\gamma (2\pi)^{\frac{3}{2}} \rho_\gamma \left(\vec{k}_1 \right) \rho_\gamma \left(\vec{k}_\gamma + \delta\vec{k} \right) \frac{1}{(2\pi)^{\frac{3}{2}}} \left(\frac{m_{\nu,1} m_{\nu,2}}{E_{\nu,1} E_{\nu,2}} \right)^{\frac{1}{2}},
\end{aligned} \tag{89}$$

where the corrections due to higher order in $\delta\vec{k}$ are ignored in the following calculations as in Sect. 3.1. The probability averaged over the initial spin per unit of particles of initial state is

$$\begin{aligned}
P &= \frac{1}{2} \int \frac{d\vec{X}_\gamma}{V(2\pi)^3} d\vec{k}_\gamma d\vec{p}_{\nu,2} \sum_{\text{spin}} |\mathcal{M}|^2 \\
&= \int \frac{d\vec{k}_\gamma}{(2\pi)^3 2E_\gamma} N_0^2(i) \left(I_0 p^0_{\nu,1} \left(p_{\nu,1} + k_1 - k_\gamma \right)^0 + I_i p^i_{\nu,1} \left(p_{\nu,1} + k_1 - k_\gamma \right)^i \right) \\
&\quad \times (4k_1 \cdot k_\gamma f_1)^2 \theta(\text{phase space}), \\
\theta(\text{phase space}) &= \theta((p_{\nu,1} + k_1)^2 - 2(p_{\nu,1} + k_1) \cdot k_\gamma), \\
N_0^2 &= \frac{1}{2} \left(\frac{G_F}{\sqrt{2}} \frac{2\alpha}{\pi} \right)^2 \frac{1}{4\pi} |N_\gamma|^2 \left(\frac{1}{\sigma_\gamma} \right)^3 \frac{1}{2E_{\nu,1}} \frac{1}{2E_1},
\end{aligned} \tag{90}$$

where V is the normalization volume of the initial state, and

$$f_1(k_1 \cdot k_\gamma) = \begin{cases} \dfrac{1}{4k_1 \cdot k_\gamma}; & \text{high energy}, \\ \dfrac{1}{2m_e^2}; & \text{low energy}, \end{cases} \tag{91}$$

where I_0 and I_i are given in Appendix E. The probability P is not Lorentz invariant and the values in the center-of-mass (CM) frame of the initial neutrino and photon and those of the general frame do not agree generally.

5.1.1. Center-of-mass frame

The phase space integral over the momentum in the CM frame

$$\vec{p}_{\nu,1} + \vec{k}_1 = 0,\ p = |\vec{p}_{\nu,1}| \tag{92}$$

is

$$\int \frac{d\vec{k}_\gamma}{(2\pi)^3 2E_\gamma} p^0 (2p - k_\gamma)^0 (4k_1 \cdot k_\gamma f_1)^2 \theta(\text{phase space}) = \frac{1}{6\pi^2} p^4;\ \text{high energy}, \tag{93}$$

$$\int \frac{d\vec{k}_\gamma}{(2\pi)^3 2E_\gamma} p^0 (2p - k_\gamma)^0 (4k_1 \cdot k_\gamma f_1)^2 \frac{1}{k_\gamma^2} \theta(\text{phase space}) = \frac{1}{12\pi^2} \left(\frac{p}{m_e}\right)^4 p^2;\ \text{low energy}. \tag{94}$$

Thus we have the probability

$$P = \frac{1}{2}\left(\frac{G_F}{\sqrt{2}}\frac{2\alpha}{\pi}\right)^2 \frac{1}{4\pi^{\frac{5}{2}}} \left(\sqrt{\sigma_\gamma}\log(\bar{\omega}T) + \frac{1}{2m_\gamma^2\sqrt{\sigma_\gamma}}\right)\frac{p^2}{12};\ \text{high energy}, \tag{95}$$

$$= \frac{1}{2}\left(\frac{G_F}{\sqrt{2}}\frac{2\alpha}{\pi}\right)^2 \frac{1}{4\pi^{\frac{5}{2}}} \frac{1}{4^3 6\pi^{\frac{5}{2}}} \sigma_\gamma^{-\frac{1}{2}} \frac{1}{\epsilon}\left(\frac{p}{m_e}\right)^4;\ \text{low energy}, \tag{96}$$

where $\bar{\omega}$ in the log term is the average ω_γ, and ϵ is the deviation of the index of refraction from unity given in Appendix C. The log term was ignored in the right-hand side of the low-energy region. We found that, in the majority of the region, $\frac{1}{\omega_\gamma E_\gamma \sqrt{\sigma_\gamma}}$ becomes much larger than $\sqrt{\sigma_\gamma}\log(\omega_\gamma T)$. Here we assume that the medium is not ionized.

5.1.2. Moving frame

In the frame $\vec{p}_{\nu,1} = (0, 0, p_{\nu,1})$, $\vec{k}_1 = (0, 0, -k_1)$, $p_{\nu,1} > k_1$ the probability in the high-energy region is

$$\begin{aligned} P &= N_0^2 \int \frac{d\vec{k}_\gamma}{(2\pi)^3 2E_\gamma} \theta((p_{\nu,1} + k_1)^2 - 2(p_{\nu,1} + k_1)k_\gamma) \\ &\quad \times \left[\left(p^0_{\nu,1}(p_{\nu,1} + k_1 - k_\gamma)^0 + p^l_{\nu,1}(p_{\nu,1} + k_1 - k_\gamma)^l\right)\left(\sigma_\gamma^2 \log\omega_\gamma T + \frac{\sigma_\gamma}{4\omega_\gamma E_\gamma}\right)\right. \\ &\quad \left. + p^i_{\nu,1}(p_{\nu,1} + k_1 - k_\gamma)^i(\sigma_\gamma^2 \log\omega_\gamma T)\right] \\ &= C_0\left(\sqrt{\sigma_\gamma}\log\omega_\gamma T + \frac{1}{\sqrt{\sigma_\gamma} m_\gamma^2}\right) p_{\nu,1}^2;\ p_{\nu,1} \gg k_1. \end{aligned} \tag{97}$$

In the low-energy region, the second term of P is given in the form

$$P = C_0' \frac{1}{\sqrt{\sigma_\gamma}\epsilon}\left(\frac{p_{\nu,1}}{m_e}\right)^4, \tag{98}$$

and the first term proportional to $p_{\nu,1}^6$ was ignored. Numerical constants C_0 and C_0' are proportional to $(\frac{G_F}{\sqrt{2}}\frac{2\alpha}{\pi})^2$. The photon effective mass in the high-energy region, m_γ, and the deviation of the refraction constant from unity in the low-energy region, ϵ, are extremely small in the dilute gas, and $P^{(d)}$ becomes large in these situations.

5.2. *Neutrino interaction with uniform magnetic field* $\nu + B \to \nu + \gamma$

The action Eq. (86) leads to coherent interactions of neutrinos with macroscopic electric or magnetic fields. These fields are expressed in SI units. Accordingly, we express the Lagrangian in SI units, summarized in Appendix D, and compute the probabilities. The magnetic field B in the z-direction is expressed by the field strength

$$F_{\mu\nu}(x) = \epsilon_{03\mu\nu} B, \tag{99}$$

and we have the action

$$S_{\nu\gamma}(B) = g_B \int d^4x \frac{\partial}{\partial x_\mu} \left(J^A_\mu(x) F_{12} \right), \tag{100}$$

where g_B is given in Appendix D. Because $S_{\nu\gamma}(B)$ is reduced to the surface term, the rate vanishes, $\Gamma_0 = 0$, but $P^{(d)} \neq 0$. Furthermore, $S_{\nu\gamma}(B)$ is not Lorentz invariant, and $P^{(d)}$ for $\nu_i \to \nu_j + \gamma$ becomes proportional to m_ν^2 of much larger magnitude than the naive expectation.

The amplitude is

$$\begin{aligned}
\mathcal{M} &= -iNg_B \int_{\lambda \geq 0} d^4x \frac{\partial}{\partial x^\mu} \left[e^{-i(p_{\nu,1} - p_{\nu,2})\cdot x} \tilde{\mathcal{M}}^\mu \right], \\
\tilde{\mathcal{M}}^\mu &= e^{i(k^0(k_\gamma)(x^0 - X^0_\gamma) - \vec{k}_\gamma \cdot (\vec{x} - \vec{X}_\gamma)) - \chi(x)} T^\mu, \\
T^\mu &= \bar{\nu}(p_{\nu,2})(1 - \gamma_5)\gamma^\mu \nu(p_{\nu,1})(\epsilon^0(\vec{k}_\gamma) k^z_\gamma - \epsilon^z(\vec{k}_\gamma) k^0_\gamma), \\
N &= \left(\frac{(2\pi)^3}{\sigma_\gamma \sigma_T^2} \right)^{\frac{1}{2}} N_\gamma \rho_\gamma(\vec{k}_\gamma) \frac{1}{(2\pi)^{\frac{3}{2}}} \left(\frac{\tilde{\omega}^0_{\nu,1} \tilde{\omega}^0_{\nu,2}}{p^0_{\nu,1} p^0_{\nu,2}} \right)^{\frac{1}{2}}, \quad \rho_\gamma(\vec{k}_\gamma) = \left(\frac{1}{(2\pi)^3 2k^0_\gamma} \frac{\hbar}{\epsilon_0} \right)^{\frac{1}{2}},
\end{aligned} \tag{101}$$

where

$$\sum_{\text{spin}} \left(T^{\mu_1} \left(T^{\mu_2} \right)^* \right) = \frac{8}{2\tilde{\omega}^0_{\nu,1} 2\tilde{\omega}^0_{\nu,2}} \left(p^{\mu_1}_{\nu,1} p^{\mu_2}_{\nu,2} - g^{\mu_1\mu_2} p_{\nu,1} p_{\nu,2} + p^{\mu_2}_{\nu,1} p^{\mu_1}_{\nu,2} \right) \left(\left(k^0_\gamma \right)^2 - \left(k^z_\gamma \right)^2 \right). \tag{102}$$

We have the probability from Eq. (46),

$$\begin{aligned}
P = \tilde{N}_0^2 g_B^2 (2\pi)^3 16 \frac{1}{2E_{\nu,1}} \frac{1}{\epsilon_0} \int \frac{d\vec{k}_\gamma}{(2\pi)^3 2E_\gamma} \left((k^0_\gamma)^2 - (k^3_\gamma)^2 \right) \\
\times (i)(I_0 p^0_{\nu,1} (p_{\nu,1} - k_\gamma)^0 + I_l p^l_{\nu,1} (p_{\nu,1} - k_\gamma)^l) \theta(\text{phase space}),
\end{aligned} \tag{103}$$

$$\theta(\text{phase space}) = \theta(\delta\omega_{12}^2 - 2p_{\nu,1} \cdot k_\gamma),$$

where $\tilde{N}_0^2 = (\pi\sigma_\gamma)^{-\frac{3}{2}}$, $\delta\omega_{12}^2 = (\tilde{\omega}^0_{\nu,1})^2 - (\tilde{\omega}^0_{\nu,2})^2$, I_0, I_l, and $I_{T,i}$ are given in Appendix E.

The convergence condition on the light-cone singularity is satisfied in the kinematical region, $\theta(\text{phase space})$. Thus the momentum satisfies

$$2 \left(p^0_{\nu,1} k^0_\gamma - p_{\nu,1} k_\gamma \cos\theta \right) \leq \delta\omega_{12}{}^2. \tag{104}$$

Solving k_γ, we have the condition for fraction $x = \frac{k_\gamma}{p_{\nu,1}}$,

$$\alpha_- \leq x \leq \alpha_+, \tag{105}$$

$$\alpha_\pm = \frac{\delta\omega_{12}^2 \pm \sqrt{\delta\omega_{12}^4 - 4 \left(\tilde{\omega}^0_{\nu,1} \right)^2 m_\gamma^2}}{2 \left(\tilde{\omega}^0_{\nu,1} \right)^2}, \tag{106}$$

where $\alpha_\pm = O(1)$. The process $\nu_i \to \nu_j + \gamma$ occurs with the probability Eq. (103) if

$$m_\gamma^2 \leq \frac{\left(\delta\omega_{12}^2\right)^2}{4\left(\tilde{\omega}_{\nu,1}^0\right)^2}, \tag{107}$$

which is satisfied in dilute gas. If the inequality Eq. (107) is not satisfied, this probability vanishes.

The probability P reflects the large overlap of initial and final states and is not Lorentz invariant. Consequently, although the integration region in Eq. (103) is narrow in the phase space determined by θ(phase space), which is proportional to the mass-squared difference, $\delta\omega_{12}^2$, the integrand is as large as p_ν^3. P becomes much larger than the value obtained from Fermi's golden rule.

5.2.1. High-energy neutrino

At high energy, Eq. (E10) is substituted. For the case that $\vec{p}_{\nu,1}$ is non-parallel to $\vec{B}$, we have

$$\begin{aligned} \frac{dP}{dx} &= \tilde{N}_0^2 g_B^2 (2\pi)^3 16 \frac{1}{\epsilon_0}\left(1-\cos^2\zeta\right)(-i) I_0 p_{\nu,1}^3 C(m_\gamma, x) \\ C(m_\gamma, x) &= -m_\gamma^2 x^4 + \left(\delta\omega_{12}^2 + m_\gamma^2\right) x^3 - \left(\tilde{\omega}_{\nu,1}^{0\,2} - \delta\omega_{12}^2\right) x^2 + \tilde{\omega}_{\nu,1}^{0\,2} x, \end{aligned} \tag{108}$$

where ζ is the angle between $\vec{p}_{\nu,1}$ and $\vec{B}$:

$$\vec{B}\cdot\vec{p}_{\nu,1} = B p_{\nu,1}\cos\zeta. \tag{109}$$

The integral I_0 is almost independent of k_γ. Ignoring the dependence, we integrate the photon's momentum, and have

$$\begin{aligned} P &= \tilde{N}_0^2 g_B^2 (2\pi)^3 16 \frac{1}{\epsilon_0}(1-\cos^2\zeta)(-i) I_0 p_{\nu,1}^3 C(m_\gamma), \\ C(m_\gamma) &= -\frac{1}{5} m_\gamma^2 \left(\alpha_+^5 - \alpha_-^5\right) + \frac{1}{4}\left(\delta\omega_{12}^2 + m_\gamma^2\right)\left(\alpha_+^4 - \alpha_-^4\right) \\ &\quad - \frac{1}{3}\left(\tilde{\omega}_{\nu,1}^{0\,2} - \delta\omega_{12}^2\right)\left(\alpha_+^3 - \alpha_-^3\right) + \frac{1}{2}\tilde{\omega}_{\nu,1}^{0\,2}\left(\alpha_+^2 - \alpha_-^2\right). \end{aligned} \tag{110}$$

The probability P of Eq. (110) is proportional to $(\tilde{\omega}_{\nu,1}^0)^2 p_{\nu,1}^3$, which is very different from the rate of the normal neutrino radiative decay, $\Gamma = G_F^2 m_\nu^5 \,(m_{\nu_1}/E_{\nu_1}) \times$ (numerical factor), especially for high-energy neutrinos. Moreover, $I_0 \propto \frac{1}{m_\gamma^2}$ can be extremely large in dilute gas, and thus P is enormously enhanced.

If the momentum of the initial neutrino is parallel to the magnetic field, $\zeta = 0$, we have

$$\begin{aligned} P &= \tilde{N}_0^2 g_B^2 (2\pi)^3 16 \frac{1}{\epsilon_0}(-i) I_0 p_{\nu,1} D(m_\gamma), \\ D(m_\gamma) &= -\left(\delta\omega_{12}^2\right)^2 \frac{\alpha_+^2 - \alpha_-^2}{2} + \delta\omega_{12}^2\left(\tilde{\omega}_{\nu,1}^0\right)^2\left(\alpha_+ - \alpha_- - 2\frac{\alpha_+^2 - \alpha_-^2}{2}\right) \\ &\quad - \left(\tilde{\omega}_{\nu,1}^0\right)^4\left(\log\frac{\alpha_+}{\alpha_-} - \alpha_+ + \alpha_-\right). \end{aligned} \tag{111}$$

P in Eq. (111) is proportional to $(\tilde{\omega}_{\nu,1}^0)^4 p_{\nu,1}$, and is negligibly small compared to that of Eq. (110).

5.2.2. Low-energy neutrino

At low energy, Eq. (E13) is substituted. I_0 is inversely proportional to k_γ^2 and we have

$$\frac{dP}{dx} = \tilde{N}_0^2 g_B^2 4\pi E_{\nu,1} \frac{1}{\epsilon_0}\left(1-\cos^2\zeta\right)\frac{1}{\epsilon}(1-x)\left[\delta\omega_{12}^2 - x m_\gamma^2 - \frac{1}{x}m_\gamma^2\right],$$

and

$$P = \tilde{N}_0^2 g_B^2 4\pi \frac{1}{\epsilon_0}(1-\cos^2\zeta)p_{\nu,1}\frac{1}{\epsilon}C_{\rm low}(m_\gamma), \tag{112}$$

$$C_{\rm low}(m_\gamma) = \delta\omega_{12}^2\left(\alpha_+ - \alpha_- - \frac{\alpha_+^2-\alpha_-^2}{2}\right) - m_\gamma^2\left(\frac{\alpha_+^2-\alpha_-^2}{2} - \frac{\alpha_+^3-\alpha_-^3}{3}\right) + \left(\tilde{\omega}_{\nu,1}^0\right)^2(\alpha_+-\alpha_-) - \left(\tilde{\omega}_{\nu,1}^0\right)^2\log\frac{\alpha_+}{\alpha_-}.$$

Using $\alpha_\pm$, $C(m_\gamma)$, $C_{\rm low}(m_\gamma)$, and $D(m)$ are computed easily.

5.3. Neutrino interaction with uniform electric field $\nu + E \to \nu + \gamma$

For a uniform electric field in the z-direction,

$$F_{\mu\nu}(x) = \frac{E}{c}\epsilon^{12\mu\nu}, \tag{113}$$

we have

$$T^\mu = \bar{\nu}(p_{\nu,2})(1-\gamma_5)\gamma^\mu\nu(p_{\nu,1})(\epsilon^x(\vec{k}_\gamma)k_\gamma^y - \epsilon^y(k_\gamma)k_\gamma^x), \tag{114}$$

$$\sum_{\rm spin}\left(T^{\mu_1}(T^{\mu_2})^*\right) = 8\frac{1}{2\tilde{\omega}_{\nu,1}^0 2\tilde{\omega}_{\nu,2}^0}\left(p_{\nu,1}^{\mu_1}p_{\nu,2}^{\mu_2} - g^{\mu_1\mu_2}p_{\nu,1}\cdot p_{\nu,2} + p_{\nu,1}^{\mu_2}p_{\nu,2}^{\mu_1}\right)\left((k_\gamma^x)^2 + (k_\gamma^y)^2\right). \tag{115}$$

$\nu_i \to \nu_j + \gamma$ in the electric field is almost the same as that in the magnetic field.

5.3.1. High-energy neutrino

We have the probability in the high-energy region,

$$P = \tilde{N}_0^2 g_E^2 (2\pi)^3 16\frac{1}{c^2\epsilon_0}(1-\cos^2\zeta)(-i)I_0 p_{\nu,1}^3 C(m_\gamma), \tag{116}$$

where the angle is defined by

$$\vec{E}\cdot\vec{p}_{\nu,1} = E p_{\nu,1}\cos\zeta. \tag{117}$$

5.3.2. Low-energy neutrino

The probability in the low-energy region is

$$P = \tilde{N}_0^2 g_E^2 4\pi\frac{1}{c^2\epsilon_0}(1-\cos^2\zeta)p_{\nu,1}\frac{1}{\epsilon}C_{\rm low}(m_\gamma). \tag{118}$$

5.4. Neutrino interaction with nucleus electric field $\nu + E_{\rm nucl} \to \nu + \gamma$

In space-time near a nucleus, there is the Coulombic electric field $E_{\rm nucl}$ due to the nucleus, and one $F_{\mu\nu}$ in the action is replaced with $E_{\rm nucl}$. The rate estimated in Ref. [36] was much smaller by a factor

of 10^{-4} or more than the value of the normal process due to charged current interaction. Here we estimate $P^{(d)}$ for the same process. The action becomes

$$S_{\nu\gamma}(E_{\rm nucl}) = \frac{1}{2\pi}\alpha\frac{G_F}{\sqrt{2}}\int d^4x \frac{\partial}{\partial x_\rho}\left(f_1 J^A_\rho(x) F_{\mu\nu}F^{\mu\nu}_{\rm nucl}\right), \tag{119}$$

which causes the unusual radiative interaction of the neutrino in matter. For the high-energy neutrino, where $2k_1\cdot k_\gamma \gg m_e^2$, we substitute the value $f_1 = \frac{1}{8m_e^2}$. Since $F^{\mu\nu}_{\rm nucl}$ due to a bound nucleus is short-range, the probability is not enhanced.

5.5. *Neutrino interaction with laser wave* $\nu + E_{\rm laser} \to \nu + \gamma$

In the scattering of a neutrino with a classical electromagnetic wave due to a laser, one $F_{\mu\nu}$ in the action is replaced with the electromagnetic field $E_{\rm laser}$ of the laser of the form

$$F^{\mu\nu}_{\rm laser} = E^i \epsilon^{0i\mu\nu} e^{ik_1\cdot x}. \tag{120}$$

The probability $P^{(d)}$ of this process is computed with the action

$$S_{\nu\gamma}(E_{\rm laser}) = \frac{1}{2\pi}\alpha\frac{G_F}{\sqrt{2}}\int d^4x \frac{\partial}{\partial x_\rho}(f_1 J^A_\rho(x) F_{\mu\nu}F^{\mu\nu}_{\rm laser}), \tag{121}$$

where $2k_1\cdot k_\gamma \approx 0$, and we substitute the value $f_1 = \frac{1}{2m_e^2}$. The amplitude and probability are almost equivalent to those of the uniform electric field. Natural unit is used in Eqs. (119) and (121).

6. Implications for neutrino reactions in matter and fields

An initial neutrino is transformed to another neutrino and a photon following the probability $P^{(d)}$. The photon in the final state interacts with a microscopic object in matter with the electromagnetic interaction, and loses energy. Thus the size σ_γ in $P^{(d)}$ is determined by its wavefunction, and the probability $P^{(d)}\times\sigma_{\gamma A}$, where $\sigma_{\gamma A}$ is the cross section of the photon and is much larger than that of weak-interaction reactions, determines the effective cross section of the whole process. Hence the effective cross section can be as large as that of the normal weak-interaction process caused by the charged current interaction.

6.1. *Effective cross section*

The probability of the event that the photon reacts on another object is expressed by $P^{(d)}$ in Eqs. (96)–(98), and that of the final photon. If a system initially has photons of density $n_\gamma(E_\gamma)$, the number of photons is multiplied, and the probability of the event that the initial neutrino is transformed is given by $P^{(d)}\times n_\gamma$. In the system of electric or magnetic fields, the initial neutrino is transformed to the final neutrino and photon. Hence $P^{(d)}\times n_\gamma$ for the former case and $P^{(d)}$ for the latter case are important parameters to be compared with the experiments.

The effective cross section, for the process where the photon in the final state interacts with atoms A of the cross section $\sigma_{\gamma A}$, is

$$\sigma^{(d)}_{\gamma A} = P^{(d)}(\gamma) n_\gamma \times \sigma_{\gamma A}, \tag{122}$$

for the former case, and

$$\sigma^{(d)}_{\gamma A} = P^{(d)}(\gamma) \times \sigma_{\gamma A}, \tag{123}$$

for the latter cases.

The cross sections Eqs. (122) and (123) are compared with that of the charged current weak process:

$$\sigma_{\nu A}^{\text{weak}} = \frac{G_F^2}{2} E_\nu M_A. \tag{124}$$

Since $\sigma_{\gamma A}$ is much larger than $\sigma_{\nu A}^{\text{weak}}$, by a factor of 10^{14} or more, $\sigma_{\gamma A}^{(d)}$ in Eqs. (122) and (123) can be as large as Eq. (124), if $P^{(d)}$ is around 10^{-14}. Accordingly, 10^{-14} or 10^{-15} is the critical value for the photon–neutrino process to be relevant and important. If the value is larger, then the reaction that is dictated to vanish due to the Landau–Yang theorem manifests with a sizable probability.

6.2. $\nu + \gamma \to \nu + \gamma$

The probability $P^{(d)}$ is of the order of αG_F and is almost independent of time. The probability in this order has been considered to be vanishing, and this process has not been studied. If the magnitude is sizable, these neutrino processes should be included in astronomy and others. The process $\nu + \bar{\nu} \to \gamma + \gamma$ is almost equivalent to $\nu + \gamma \to \nu + \gamma$, and we do not study it in this paper.

A system of high temperature has many photons, and a neutrino makes a transition through its collision with the photons. The probability is determined by the product between the number of photons n_γ and each probability:

$$P^{(d)}(\gamma) n_\gamma. \tag{125}$$

In a thermal equilibrium of higher temperature, the density is about

$$n_\gamma = (k_B T)^3, \tag{126}$$

and we have the product for a head-on collision

$$P n_\gamma = (G_F \alpha)^2 \frac{2}{8\pi^{9/2} m_\gamma^2 \sigma_\gamma^{1/2}} \frac{p_\nu^2}{12} (k_B T)^3. \tag{127}$$

The probability is inversly proportional to m_γ^2, and is enhanced enormously for small m_γ, which is realized in a dilute gas.

6.2.1. *The sun*

In the core of the sun,

$$R = 10^9 \text{ m}, \tag{128}$$
$$k_B T \approx 2 \text{ keV},$$

and the solar neutrino has an energy around 1–10 MeV. The photon's energy distribution is given by the Planck distribution, and the mean free path for the head-on collision is

$$l = \frac{1}{P^{(d)}(\gamma) n_\gamma n_A \sigma_{\gamma A}} = 5 \times 10^{15} \text{ m}, \tag{129}$$

where $\sigma_{\gamma A} = 10^{-24} \text{ cm}^2$, $m_\gamma = 1 \text{ eV}$, and $n_A = 10^{29}/\text{cm}^3$ are used. The value is much larger than the sun's radius.

For a neutrino of higher energy, we use Eq. (97), and have

$$l = \frac{1}{P^{(d)}(\gamma) n_\gamma n_A \sigma_{\gamma A}} = 6.2 \times 10^9 \left(\frac{p_\nu^0}{p_\nu} \right)^2 \text{ m}, \tag{130}$$
$$p_\nu^0 = 10 \text{ GeV};$$

thus, the length exceeds the sun's radius for $p_\nu < 25 \text{ GeV}$. The high-energy neutrino does not escape from the core if the energy is higher than around 25 GeV.

6.2.2. Supernovae

In supernovae, the temperature is as high as 10 MeV and the probability becomes much higher. We have

$$l = \frac{1}{P^{(d)}(\gamma) n_\gamma n_A \sigma_{\gamma A}} = 1\,\mathrm{m}, \tag{131}$$
$$\frac{p_\gamma}{m_\gamma} = 10^7, \quad n_A = 10^{25}/\mathrm{cm}^3,$$

or

$$l = 10^4\,\mathrm{m}, \tag{132}$$
$$\frac{p_\gamma}{m_\gamma} = 10^5,\ n_A = 10^{24}/\mathrm{cm}^3.$$

The mean free path becomes shorter in the lower matter density region. Thus in the region of small photon effective mass, the neutrino does not escape but loses the majority of its energy. This is totally different from the standard behavior of the supernova neutrino.

6.2.3. Neutron star

If magnetic field is as high as 10^9 T, then the probability becomes large. The energy of the neutrino is transfered to the photon's energy.

6.2.4. Low-energy reaction

In the low-energy region, $P^{(d)}$ behaves as Eq. (96) and

$$\sigma_{\gamma A} \to C E_{\mathrm{photon}}^{-3.5}, \quad E_{\mathrm{photon}} \to 0. \tag{133}$$

The effective transition probability $P^{(d)} n_\gamma$ and the cross section depend on the photon density.

6.3. $\nu + (E, B) \to \nu' + \gamma$

The radiative transition of one neutrino to another lighter neutrino and photon in the electromagnetic field occurs with the probability $P^{(d)}$. Because $P^{(d)}$ is not proportional to T but almost constant, the number of parents decreases fast at small T, and remains the same afterward without decreasing. Now the photon in the final state reacts with matter with sizable magnitude and the probability of the whole process is expressed with the effective cross section.

6.3.1. High-energy neutrinos

The transition probability of the high-energy neutrino in the magnetic field B (T) and electric field E (V/m) are

$$P_B = 4\alpha \left(\frac{ecB}{m_e c^2}\right)^2 \frac{G_F^2}{2} \pi^{-\frac{3}{2}} \frac{1}{4m_\gamma^2 \sqrt{\sigma_\gamma}} p_\nu^3 C(m_\gamma) \frac{1}{m_e^2}, \tag{134}$$

$$P_E = 4\alpha \left(\frac{eE}{m_e c^2}\right)^2 \frac{G_F^2}{2} \pi^{-\frac{3}{2}} \frac{1}{4m_\gamma^2 \sqrt{\sigma_\gamma}} p_\nu^3 C(m_\gamma) \frac{1}{m_e^2}. \tag{135}$$

For the parameters

$$m_\gamma c^2 = 10^{-9}\,\mathrm{eV}, \quad \sqrt{\sigma_\gamma} = 10^{-13}\,\mathrm{m} \tag{136}$$

and the neutrino mass around $0.08\,\mathrm{eV}/c^2$ [53], these are estimated numerically as

$$P_B = 6.4\times 10^{-27}\left(\frac{B}{B_0}\right)^2\left(\frac{p_\nu}{p_\nu^{(0)}}\right)^3, \tag{137}$$
$$p_\nu^{(0)} = 10\,\mathrm{MeV}, \quad B_0 = 1\,\mathrm{T},$$

and

$$P_E = 2.8\times 10^{-20}\left(\frac{E}{E_0}\right)^2\left(\frac{p_\nu}{p_\nu^{(0)}}\right)^3, \tag{138}$$
$$p_\nu^{(0)} = 10\,\mathrm{MeV}, \quad E_0 = 10^3\,\mathrm{GV/m}.$$

6.3.2. Low-energy neutrinos

The transition probabilities of the low-energy neutrino are

$$P_B = 4\alpha\left(\frac{ecB}{m_e c^2}\right)^2\frac{G_F^2}{2}\pi^{-\frac{3}{2}}\frac{1}{\epsilon\sqrt{\sigma_\gamma}}p_\nu C(m_\gamma)\frac{1}{m_e^2} \tag{139}$$

$$P_E = 4\alpha\left(\frac{eE}{m_e c^2}\right)^2\frac{G_F^2}{2}\pi^{-\frac{3}{2}}\frac{1}{\epsilon\sqrt{\sigma_\gamma}}p_\nu C(m_\gamma)\frac{1}{m_e^2}. \tag{140}$$

In the typical situations

$$\epsilon = 10^{-20}, \quad \sqrt{\sigma_\gamma} = 10^{-13}\,\mathrm{m}, \quad p_\nu = 1\,\mathrm{eV}, \quad E_0 = 10^3\,\mathrm{GV/m},$$

that is estimated as

$$P_E = 6.4\times 10^{-38}\left(\frac{E}{E_0}\right)^2. \tag{141}$$

In the overlap region, the phases of waves become canceled along the light-cone at small m_γ or ϵ, and more waves are then added constructively. Consequently, the P_B and P_E are proportional to m_γ^{-2} at high energy and ϵ^{-1} in low energy and m_ν^2, and hence are enhanced enormously compared with that of the normal radiative decay, which is due to the neutrino magnetic moment. The probabilities in Figs. 3 ($\nu + B$) and 4 ($\nu + E$) express Eqs. (137) and (138), and show the steep rise with the energy and the enhancement.

6.4. Table of processes

$P^{(d)}$ can be tested in various neutrino processes over a wide energy range; see Table 1. Using these parameters of Table, $P^{(d)}$ are estimated.

The diffractive term $P^{(d)}$ becomes substantial in magnitude at high energy or fields. So this process may be relevant to neutrinos of high energy or at high fields, and may give new insights into or measurability of the following processes.

(1) The accelerator neutrino has high energy and total intensity of the order 10^{20}. At $B = 10\,\mathrm{T}$ and $P_\nu = 1(10)\,\mathrm{GeV}$, we have $P \approx 10^{-18}(10^{-15})$, and, using a laser of $E_0 = 10^3\,\mathrm{GV/m}$ at $P_\nu = 1(10)\,\mathrm{GeV}$, we have $P \approx 10^{-16}(10^{-13})$. The neutrino from the accelerator may be probed by detecting the final gamma rays. For example, at the beam dump of LHC we may set up a laser to detect the neutrino interaction.

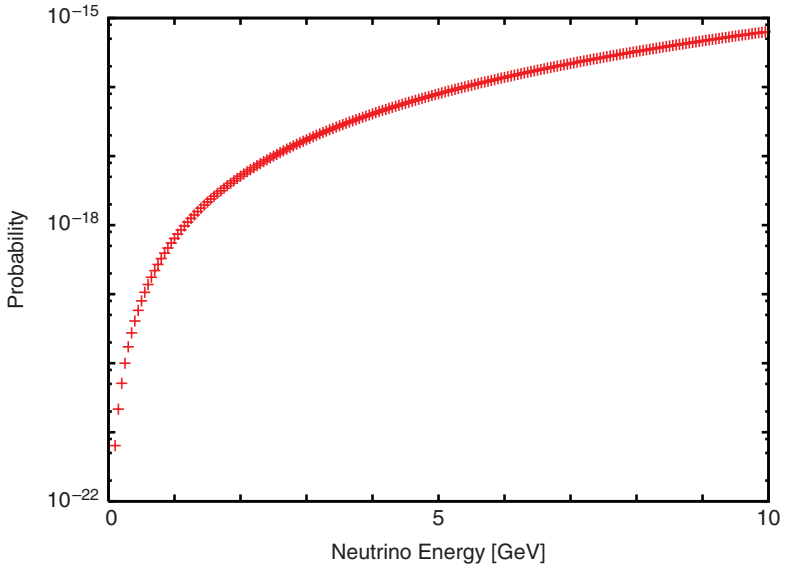

Fig. 3. E_ν dependence of the probability Eq. (137) is shown. $B = 10$ T is used for the calculation.

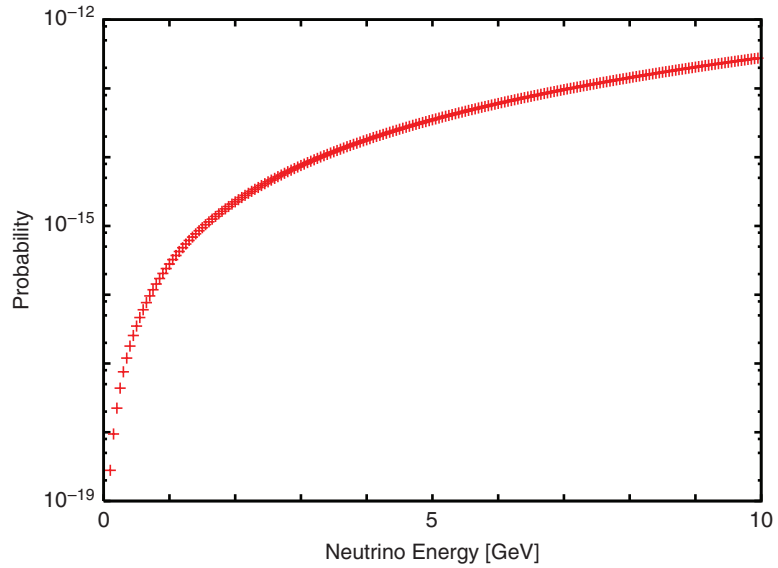

Fig. 4. E_ν dependence of the probability Eq. (138) is shown. $E = 100\,\mathrm{GV/m}$ is used for the calculation.

(2) For a reactor neutrino, of a flux $\approx 10^{20}$/s per reactor, a detector of high magnetic field of the order 10 T, or of high-intensity laser, may be able to detect the neutrino.
(3) Direct observations of solar neutrinos, which have an energy of 0.5–10 MeV and flux around $10^{15}/\mathrm{m}^2$ s, using a detector with a strong magnetic field, similar to that for the axion search [54], would be possible.
(4) In a supernova or neutron star, the neutrino–photon reaction would give a new important process, because the final photon strongly interacts with matter. As to the detectability of neutrinos from the sun, 10 GeV is the threshold from the sun, while those from supernovae interact with 10 MeV photons.

Table 1. Physical parameters of neutrinos on various processes are shown.

Neutrino source	Energy	Flux	B	E
Solar neutrino	1–10 MeV	$10^{15}/\mathrm{m}^2\,\mathrm{s}$	1–5 T	–
Reactor neutrino	3–8 MeV	$10^{20}/\mathrm{s}$	1–5 T	–
Cumulonimbus cloud	1–10 MeV	$10^{15}/\mathrm{m}^2\,\mathrm{s}$ (solar ν)	10^{-5} T	10^3 GV/m
Accelerator neutrino	0.5–50 GeV	10^{20}	1–5 T	–
Cosmic neutrino	$\sim 10^6$ GeV	$10^{-9}\,\mathrm{GeV/cm}^2\,\mathrm{s\,sr}$	10^{-5} T	–
Relic neutrino	1 meV	10^{20}/year	–	10^5 GV/m

(5) We find that $P^{(d)}$ becomes maximum at $\zeta = \frac{\pi}{2}$ from Eq. (118), and may apply this effect to enhance the neutrino flux. The term also has momentum dependence, which may be exploited for an "optical" effect of neutrinos through the photon interaction.

(6) The photon–neutrino reaction may be useful for relic neutrino detection. The reaction rate may be enhanced with such methods as the neutrino mirrors that collect them (Ref. [55] and J. Arafune and G. Takeda, private communication). We may take advantage of the above effect.

(7) The probability becomes huge at extremely high energies. So, this process may be relevant to the ultra-high-energy neutrino process [56–58].

(8) Neutrinos may interact with electromagnetic fields in cumulonimbus clouds.
   (a) Lightning has total energy of the order 900 MJ $\approx 10^9$ CV and current 10^6 A in a short period. cB at a radius $r = 1$ cm is 1.5×10^9 N/C. Assuming that $E = cB = 1.5 \times 10^9$ N/C, and $m_\gamma c^2 = 10^{-11}$ eV, $p_\nu = 10$ MeV, we have $P_{E+B} \approx 10^{-15}$. The neutrino inevitably loses its energy, and photons of the continuous spectrum are emitted. This may be related to upper-atmospheric lightning [59,60].
   (b) The gamma rays observed in cumulonimbus clouds [61,62] may be connected with the diffractive component.

(9) Primordial magnetic fluctuations with zero frequency [63] may have interacted with neutrinos before neutrino detachment from the hot neutrino plasma (>GeV temperature) during the Big Bang. Such signatures may be carried by neutrinos (which are now relic neutrinos).

7. Summary and future prospects

We have found that the photon interaction expressed by the total derivative Eqs. (13) or (86), which are derived from the triangle diagram in the standard model, causes unusual transitions characterized by the time-independent probability. The interaction Lagrangian of this form does not give rise to any physical effect in classical physics, because the equation of motion is not affected. In quantum mechanics, this assertion is correct for the transition rate Γ_0. However, this does not apply to the diffractive term $P^{(d)}$, which manifests the wave characteristics of the initial and final waves. Our results show that $P^{(d)}$ is relevant to experiments and important in understanding many phenomena in nature.

Neutral particles do not interact with the photon in classical mechanics. In quantum field theory, the vacuum fluctuation expressed by the triangle diagram gives the effective interaction to the neutral particles such as 1^+ meson $\to \gamma\gamma$ and $\nu + \gamma(B, E) \to \nu + \gamma$. However, they have vanishing rates due to the Landau–Yang–Gell-Mann theorem. $P^{(d)}$ does not vanish, nevertheless, and holds unusual properties such as the violation of the kinetic-energy conservation and that of Lorentz invariance. Furthermore, the magnitudes become comparable to or even larger than the normal weak-interaction

processes. Accordingly, the two-photon or two-gluon decays of the neutral axial vector mesons composed of a pair of electrons or quarks come to have finite decay probabilities. They will be tested in experiments. The neutrino–photon processes, which have been ignored, also have finite probabilities from $P^{(d)}$. It will be interesting to observe the neutrino–photon processes directly using electric or magnetic fields, or laser and neutrino beams in various energy regions. The diffractive probability $P^{(d)}$ will also be important in understanding the wide-ranging neutrino processes in the earth, stars, astronomy, and cosmology.

The diffractive probability $P^{(d)}$ is caused by the overlap of wavefunctions of the parent and decay products, which makes the interaction energy finite and the kinetic energy vary. Consequently, the final state has continuous spectrum of the kinetic energy and possesses a wave nature unique to the waves. The unique feature of $P^{(d)}$, i.e., independence of the time interval T, shows that the number of parents, which decrease as $e^{-\Gamma T}$ in the normal decay, is now constant. The states of parent and daughter are expressed by quasi-stationary states, which are expressed by the superposition of different energies and are different from the normal stationary state of the form $e^{\frac{-iEt}{\hbar}}\psi(\vec{x})$.

The probability of the events in which neutrinos or photons are detected is computed with $S[T]$, which satisfies the boundary condition of the physical processes. Applying $S[T]$, we have obtained results that can be compared with experiments. The pattern of the probability is determined by the difference of angular velocities, $\omega = \omega^E - \omega^{dB}$, where $\omega^E = E/\hbar$ and $\omega^{dB} = c|\vec{p}|/\hbar$. The quantity ω takes the extremely small value $m^2c^4/(2E\hbar)$ for light particles such as neutrinos or photons in matter [51]. Consequently, the diffractive term becomes finite in the macroscopic spatial region of $r \leq \frac{2\pi E\hbar c}{m^2c^4}$, and the probabilities Eqs. (95)–(98), (110), (112), (116), and (118) become extremely large for small m and large E.

This allows us to introduce a new class of experimental measurement possibilities of the deployment of photons to detect weakly interacting particles such as neutrinos. Because of the modern technology of electric and magnetic fields and lasers, a large number of coherent photons are possible and the effects we have derived may have important implications in detecting and enhancing the measurement of neutrinos with photons. We see a variety of detectability opportunities that have eluded attention till now. These happen either with high-energy neutrinos, such as those from cosmic rays and accelerators, or in high fields (such as intense laser and strong magnetic fields). In the latter examples, neutrinos from reactors, accelerators, the sun, supernovae, thunder clouds, and even polar ice may be detected with enhanced probabilities using intense lasers. We also mention the probability estimate for primordial relic neutrinos and embedded information in them.

The physical processes in nature follow the probabilities thus computed, even though the measurements have not been made. Accordingly, those probabilities $P^{(d)}$ that are obtained in the present paper are invaluable for understanding natural phenomena.

Acknowledgements

This work was partially supported by a Grant-in-Aid for Scientific Research (Grant No. 24340043) and by the Norman Rostoker Fund. The authors thank Dr Atsuto Suzuki, Dr Koichiro Nishikawa, Dr Takashi Kobayashi, Dr Takasumi Maruyama, Dr Tsuyoshi Nakaya, and Dr Fumihiko Suekane for useful discussions on the neutrino experiments, and Dr Shoji Asai, Dr Tomio Kobayashi, Dr Toshinori Mori, Dr Sakue Yamada, Dr Kensuke Homma, Dr Masashi Hazumi, Dr Kev Abazajian, Dr S. Barwick, Dr H. Sobel, Dr M. C. Chen, Dr P. S. Chen, Dr M. Sato, Dr H. Sagawa, and Dr Y. Takahashi for useful discussions.

Appendix A.

Wavefunctions including CG coefficients are

$$\phi_0 : |J=0, \vec{P}=0\rangle = \frac{1}{\sqrt{3}}\left|\frac{1}{2},\frac{1}{2};-1\right\rangle - \frac{1}{\sqrt{6}}\left|\frac{1}{2},-\frac{1}{2};-1\right\rangle + \frac{1}{\sqrt{6}}\left|-\frac{1}{2},\frac{1}{2};-1\right\rangle + \frac{1}{\sqrt{3}}\left|-\frac{1}{2},-\frac{1}{2};-1\right\rangle, \tag{A1}$$

$$\phi_1 : |J=1, \vec{P}=0\rangle = \frac{1}{\sqrt{2}}\left|\frac{1}{2},\frac{1}{2};0\right\rangle - \frac{1}{2}\left|\frac{1}{2},-\frac{1}{2};-1\right\rangle - \frac{1}{2}\left|-\frac{1}{2},\frac{1}{2};1\right\rangle, \tag{A2}$$

$$\phi_2 : |J=2, \vec{P}=0\rangle = \left|\frac{1}{2},\frac{1}{2};1\right\rangle. \tag{A3}$$

Appendix B.

The integration over a semi-infinite region satisfying the causality in 2D variables, $x_1(t_1, x_1)$ and $x_2(t_2, x_2)$,

$$I = \int_{\lambda_1,\lambda_2\geq 0} d^2x_1 d^2x_2 \frac{\partial}{\partial t_1}\frac{\partial}{\partial t_2} f(x_1 - x_2) g(x_1 + x_2), \tag{B1}$$

where the integrands satisfy

$$g(t_+, x_+ = \pm\infty) = 0, \;\; f(t_-, x_- = \pm\infty) = 0, \tag{B2}$$

is made with the change of variables. Due to Eq. (B2), I would vanish if the integration region were from $-\infty$ to $+\infty$. We write I with variables $x_+ = \frac{x_1+x_2}{2}$, $x_- = x_1 - x_2$, and have

$$I = I_1 - I_2, \tag{B3}$$

$$I_1 = \int_{\lambda_+\geq 0} d^2x_- f(x_-) d^2x_+ \frac{\partial^2}{\partial t_+^2} g(x_+),$$

$$I_2 = \int_{\lambda_+\geq 0} d^2x_+ g(x_+) d^2x_- \frac{\partial^2}{\partial t_-^2} f(x_-),$$

where $\lambda_+ = x_+^2$. It is noted that x_+ is integrated in the restricted region but x_- is integrated in the whole region. Thus

$$I_1 = -\int d^2x_- f(x_-) dt_+ v^2 \left.\frac{\partial}{\partial x_+} g(x_+)\right|_{x_+ = x_{+,\min}},$$

$$I_2 = 0, \tag{B4}$$

where the functional form $g(x_+) = g(x_+ - vt_+)$ was used. I is computed with the slope of $g(x_+)$ at the boundary $x_+ = t_+$. We apply this method for computing 4D integrals.

Appendix C.

In the case of the low-energy region, the photon has no effective mass, but is expressed by the index of refraction very close to unity in dilute gas,

$$n = 1 + \epsilon. \tag{C1}$$

Accordingly, the angular velocity in $\bar{\phi}_c(\delta t)$ is given by

$$\omega = (1+\epsilon)k_\gamma - k_\gamma = \epsilon k_\gamma. \tag{C2}$$

ϵ in air is

$$\epsilon = 0.000\,292, \quad 0\,^\circ\mathrm{C}, \quad 1 \text{ atmospheric pressure}, \tag{C3}$$

and ϵ in dilute gas becomes extremely small, of the order 10^{-14}–10^{-15}. Consequently, the integrand in $P^{(d)}$ is proportional to $2/(k_\gamma \epsilon)$.

Appendix D. Notation: SI units

It is convenient to express the Lagrangian with SI units to study quantum phenomena caused by macroscopic electric and magnetic field [64]. The Maxwell equations for electric and magnetic fields are expressed with the dielectric constant and magnetic permeability of the vacuum, ϵ_0 and μ_0, which are related to the speed of light, c,

$$c = \frac{1}{\sqrt{\epsilon_0 \mu_0}}. \tag{D1}$$

The zeroth component x_0 in 4D coordinates x_μ is

$$x_0 = ct; \quad t = \mathrm{s}. \tag{D2}$$

The Maxwell equations in vacuum are

$$\begin{aligned}
&\vec{\nabla} \cdot \vec{E} = \frac{1}{\epsilon_0}\rho(x), \\
&\vec{\nabla} \cdot \vec{B} = 0, \\
&\vec{\nabla} \times \frac{\vec{E}}{c} = -\frac{\partial \vec{B}}{\partial x_0}, \\
&\vec{\nabla} \times \vec{B} = \mu_0 \vec{j}(x) + \frac{1}{c}\frac{\partial \vec{E}}{\partial x_0},
\end{aligned} \tag{D3}$$

where the charge density and electric current, $\rho(x)$ and $\vec{j}(x)$, satisfy

$$c\frac{\partial}{\partial x_0}\rho(x) + \vec{\nabla} \cdot \vec{j}(x) = 0. \tag{D4}$$

Using the vector potential

$$A_\mu = (A_0, -\vec{A}), \tag{D5}$$

we write

$$\begin{aligned}
&\frac{1}{c}\vec{E}(x) = -\frac{\partial}{\partial x_0}\vec{A}(x) - \vec{\nabla} A_0(x), \\
&\vec{B} = \vec{\nabla} \times \vec{A}(x),
\end{aligned} \tag{D6}$$

and the Lagrangian density of electric and magnetic fields

$$L_{\mathrm{EM}} = -\frac{1}{4}\frac{1}{\mu_0}F_{\mu\nu}F^{\mu\nu} = \frac{\epsilon_0}{2}\vec{E}^2 - \frac{1}{2\mu_0}\vec{B}^2. \tag{D7}$$

The Lagrangian density of electronic fields is,

$$L_e = \bar{\psi}(x)\left[\gamma_0 i c\hbar\frac{\partial}{\partial x_0} - \gamma_l i c\hbar\frac{\partial}{\partial x_l} - mc^2\right]\psi, \tag{D8}$$

and that of QED is

$$L_{\mathrm{QED}} = L_e + L_{\mathrm{EM}} + ecA_0\bar{\psi}\gamma_0\psi - ecA_l\bar{\psi}\gamma_l\psi. \tag{D9}$$

Canonical momenta and commutation relations from Eqs. (D7) and (D9) are

$$\pi_\psi(x) = \frac{\partial}{\partial\dot{\psi}(x)}L = i\hbar\psi^\dagger(x), \tag{D10}$$

$$\Pi_l(x)(x) = \frac{\partial}{\partial\dot{A}_i(x)}L = \frac{1}{\mu_0 c^2}E_i,$$

$$\{\psi(x_1), \psi^\dagger(x_2)\}\delta(t_1 - t_2) = \delta(\vec{x}_1 - \vec{x}_2)\delta(t_1 - t_2),$$

$$[A_i(x_1), \dot{A}_j(x_2)]\delta(t_1 - t_2) = i\frac{\hbar}{\epsilon_0}\delta_{ij}\delta(\vec{x}_1 - \vec{x}_2)\delta(t_1 - t_2), \tag{D11}$$

where the gauge-dependent term is ignored in the last equation. Thus the commutation relations for electron fields do not have $\hbar$, and those of electromagnetic fields have $\hbar$ and the dielectric constant ϵ_0. $\frac{\hbar}{\epsilon_0}$ shows the unit size in phase space. Accordingly, the number of states per unit area and the strength of the light-cone singularity are proportional to $1/\epsilon_0$. The fields are expanded with the wave vectors as

$$\psi(x) = \sum_s \int \frac{d\vec{k}}{\sqrt{(2\pi)^3}}\sqrt{\frac{\tilde{\omega}_0}{k^0(\vec{k})}}(u(\vec{k}, s)b(\vec{k}, s)e^{-ik\cdot x} + v(\vec{k}, s)d^\dagger(\vec{k}, s)e^{ik\cdot x}), \tag{D12}$$

$$A_i(x) = \sum_s \int \frac{d\vec{k}}{\sqrt{((2\pi)^3 2k_0)}}\sqrt{\frac{\hbar}{\epsilon_0}}(\epsilon_i(\vec{k}, s)a(\vec{k}, s)e^{-ik\cdot x} + \epsilon_i^*(\vec{k}, s)a^\dagger(\vec{k}, s)e^{ik\cdot x}), \tag{D13}$$

where

$$k\cdot x = k_0 x_0 - \vec{k}\cdot\vec{x},$$

$$k_0(\vec{k}) = \sqrt{\vec{k}^2 + \tilde{\omega}_0^2}, \quad \tilde{\omega}_0 = \frac{mc}{\hbar}. \tag{D14}$$

The creation and annihilation operators satisfy

$$\{b(\vec{k}_1, s_1), b^\dagger(\vec{k}_2, s_2)\} = \delta(\vec{k}_1 - \vec{k}_2)\delta_{s_1 s_2}, \tag{D15}$$

$$[a(\vec{k}_1, s_1), a^\dagger(\vec{k}_2, s_2)] = \delta(\vec{k}_1 - \vec{k}_2)\delta_{s_1 s_2}. \tag{D16}$$

The spinor is normalized as

$$\sum_s u(\vec{k}, s)\bar{u}(\vec{k}, s) = \frac{\gamma\cdot k + \tilde{\omega}_0}{2\tilde{\omega}_0}, \tag{D17}$$

and the light-cone singularity is

$$\Delta_+(x_1 - x_2) = \int \frac{d\vec{k}}{(2\pi)^3 2k_0}e^{-ik\cdot(x_1 - x_2)} = 2i\frac{1}{4\pi}\delta(\lambda)\epsilon(\delta x^0) + \cdots, \tag{D18}$$

where the less-singular and regular terms are in $\cdots$.

The action

$$S = \int dx(L_{\rm QED} + \bar{\psi}(x)\gamma_\mu(1 - \gamma_5)\psi(x)J^\mu(x)),$$

$$J^\mu(x) = \frac{G_F}{\sqrt{2}}\bar{\nu}(x)\gamma^\mu(1 - \gamma_5)\nu(x) \tag{D19}$$

governs the dynamics of the electron, photon, and neutrino. Integrating $\psi(x)$ and $\bar{\psi}(x)$, we have $\mathrm{Det}(D + J^\mu\gamma_\mu(1 - \gamma_5))$ and the effective action between the neutrino and photon

$$S_{\rm eff} = \frac{e^2}{8\pi^2 c\hbar^2}f(0)\int dx\frac{\partial}{\partial x^\nu}\left[J^\nu(x)\epsilon_{\alpha\beta\rho\sigma}\frac{\partial}{\partial x_\alpha}A^\beta\frac{\partial}{\partial x_\rho}A^\sigma\right], \tag{D20}$$

where

$$f(0) = \frac{1}{2\tilde{\omega}_0^2}. \tag{D21}$$

The magnetic and electric fields in the third direction, and laser field expressed by the external fields

$$F_{\rm ext}^{\mu\nu} = \epsilon^{03\mu\nu} B,\ F_{\rm ext}^{\mu\nu} = \epsilon^{12\mu\nu} \frac{E}{c},\ A_{\rm laser}^{\mu}(x) \tag{D22}$$

are substituted into the action Eq. (D20), and we have the actions

$$S_{{\rm eff},B} = g_B \epsilon_{03\rho\sigma} \int dx \frac{\partial}{\partial x^\nu} \left[\bar{\nu}(x) \gamma^\nu (1-\gamma_5) \nu(x) \frac{\partial}{\partial x_\rho} A^\sigma(x) \right], \tag{D23}$$

$$S_{{\rm eff},E} = g_E \epsilon_{12\rho\sigma} \int dx \frac{\partial}{\partial x^\nu} \left[\bar{\nu}(x) \gamma^\nu (1-\gamma_5) \nu(x) \frac{\partial}{\partial x_\rho} A^\sigma(x) \right], \tag{D24}$$

$$S_{\rm eff,laser} = g_l \epsilon_{\mu\nu\rho\sigma} \int dx \frac{\partial}{\partial x^\nu} \left[\bar{\nu}(x) \gamma^\nu (1-\gamma_5) \nu(x) F_{\rm laser}^{\mu\nu}(x) \frac{\partial}{\partial x_\rho} A^\sigma(x) \right], \tag{D25}$$

where the coupling strengths are

$$g_B = \frac{e^2}{8\pi^2 c\hbar^2} f(0) B \frac{G_F}{\sqrt{2}}, \tag{D26}$$

$$g_E = \frac{e^2}{8\pi^2 c\hbar^2} f(0) \frac{E}{c} \frac{G_F}{\sqrt{2}}, \tag{D27}$$

$$g_l = \frac{e^2}{8\pi^2 c\hbar^2} f(0) \frac{G_F}{\sqrt{2}}. \tag{D28}$$

The wave vectors are connected with the energy and momentum

$$E(\vec{k}) = \hbar c k_0(\vec{k}), \quad \vec{p} = \hbar c \vec{k}. \tag{D29}$$

Appendix E. Integration formulae

The integrals

$$I_0 = \int_{\lambda_+=0} d^4x_1 d^4x_2 \rho_s(x_-^0) \left(\frac{\partial}{\partial x_+^0} \right)^2 e^{-\chi(x_1)-\chi(x_2)^*} \delta(\lambda_-) e^{ip\cdot x_-}, \tag{E1}$$

$$I_i = \int_{\lambda_+=0} d^4x_1 d^4x_2 \rho_s(x_-^0) \left(\frac{\partial}{\partial x_+^i} \right)^2 e^{-\chi(x_1)-\chi(x_2)^*} \delta(\lambda_-) e^{ip\cdot x_-}, \tag{E2}$$

$$\rho_s(x_-^0) = 1 + i \frac{x_1^0 - x_2^0}{E_\gamma \sigma_\gamma},$$

where the spreading in the transverse direction in Eq. (58) leads to $\rho_s(x_-^0)$ on the right-hand sides, are evaluated hereafter. Changing the variables to x_+ and x_-, we have

$$\begin{aligned}
\chi(x_1) + \chi(x_2)^* &= \chi^{(+)}(x_+) + \chi^{(-)}(x_-) + \chi^{(+-)}(x_+, x_-), \\
\chi^{(+)}(x_+) &= \frac{1}{\sigma_\gamma}((x_{+,l} - v(x_{+,0}))^2 + \frac{1}{2\sigma_T(+)}((\vec{x}_+)_T^2), \\
\chi^{(-)}(x_-) &= \frac{1}{4\sigma_\gamma}(x_{-,l} - v(x_{-,0}))^2 + \frac{1}{8\sigma_T(+)}((\vec{x}_-)_T^2), \\
\chi^{(+-)}(x_+, x_-) &= \frac{1}{\sigma_T(-)}((\vec{x}_+)_T(\vec{x}_-)_T),
\end{aligned} \tag{E3}$$

where the wavepacket sizes in the transverse direction are

$$\frac{1}{2\sigma_T(+)} = \frac{1}{2\sigma_T(1)} + \frac{1}{2\sigma_T(2)^*},$$
$$\frac{1}{2\sigma_T(-)} = \frac{1}{2\sigma_T(1)} - \frac{1}{2\sigma_T(2)^*}. \tag{E4}$$

The wavepacket expands in the transverse direction and the size $\sigma_T(+)$ is given by

$$\sigma_T(+) = \frac{\sigma_\gamma}{2} - \frac{i}{4E}(x_-^0) + O(x_-^2, x_+^2). \tag{E5}$$

The off-diagonal term $\chi(x_+, x_-)$ gives small corrections and is ignored. We have

$$I_0 = \frac{1}{\sigma_\gamma} I_0(+) I(-),$$
$$I_0(+) = -\int_{x_+^0=|\vec{x}_+|} dx_l^+ d^2\vec{x}_T^+ e^{-\chi(x_+)} \frac{(\vec{x}_T^+)^2}{x_l^+} = -\int dx_+^l \pi (2\sigma_T(+))^2 \frac{1}{x_+^l},$$
$$I(-) = \int d^4x_- \rho(x_-^0) e^{-\chi(x_-)} \delta(\lambda_-^2) e^{ip\cdot x_-} = \int dx_-^0 \rho(x_-^0) \frac{4\sigma_T(+)}{x_-^0} e^{i\omega_\gamma x_-^0}, \tag{E6}$$

and

$$I_0 = -\pi \int_0^T dx_+^l \frac{1}{x_+^l} \int_{-x_+^l}^{+x_+^l} dx_-^0 \rho(x_-^0) \frac{16\sigma_T(+)^3}{\sigma_\gamma} \frac{e^{i\omega_\gamma x_-^0}}{x_-^0}$$
$$= i2\pi^2 \left(\sigma_\gamma^2 \log(\omega_\gamma T) + \frac{\sigma_\gamma}{4\omega_\gamma E_\gamma} \right). \tag{E7}$$

Equation (E7) is composed of the $\log T$ term and a constant. At $\omega_\gamma \approx 0$, the latter is important and, at larger ω_γ, the former is important.

Similarly,

$$I_i = I_i(+) I(-)$$
$$I_i(+) = \int_{x_+}^{i} = \pm\sqrt{(x_+^0)^2 - (x_+^l)^2 - (x_+^i)^2} dx_+^0 dx_+^l d\vec{x}_+^{i'} \frac{x_+^i}{\sigma_T(+)} e^{-\chi(x_+)}$$
$$= -\pi \int dx_+^0 \frac{2\sigma_T(+)}{x_+^0}, \tag{E8}$$

and

$$I_i = -\pi \int_0^T dx_+^0 \frac{1}{x_+^0} \int_{x_+^0}^{x_+^0} dx_-^0 \rho(x_-^0) 8\sigma_T(+)^2 \frac{e^{i\omega_\gamma x_-^0}}{x_-^0}$$
$$= i2\pi^2 \left(\sigma_\gamma^2 \log(\omega_\gamma T) \right). \tag{E9}$$

In high-energy regions, $\omega_\gamma = \frac{m_\gamma^2}{2E_\gamma}$, and

$$I_0 = i2\pi^2 \left(\sigma_\gamma^2 \log(\omega_\gamma T) + \frac{\sigma_\gamma}{4m_\gamma^2} \right), \tag{E10}$$

$$I_{T,i} = i2\pi^2 \left(\sigma_\gamma^2 \log(\omega_\gamma T) \right), \tag{E11}$$

$$I_l = I_0. \tag{E12}$$

In low-energy regions, $\omega_\gamma = \epsilon p_\gamma$, and

$$I_0 = i2\pi^2 \left(\sigma_\gamma^2 \log(\omega_\gamma T) + \frac{\sigma_\gamma}{4\epsilon p_\gamma^2} \right), \tag{E13}$$

$$I_i = i2\pi^2 \left(\sigma_\gamma^2 \log(\omega_\gamma T) \right), \tag{E14}$$

$$I_l = I_0. \tag{E15}$$

Funding

Open Access funding: SCOAP[3].

References

[1] K. Ishikawa and Y. Tobita, Prog. Theor. Exp. Phys. **2013**, 073B02 (2013).
[2] K. Ishikawa and Y. Tobita, Ann. Phys. **344**, 118 (2014).
[3] J. J. Sakurai, *Advanced Quantum Mechanics* (Addition Wesly Pub., New York, 1967), p. 184.
[4] R. Peierls, *Surprises in Theoretical Physics* (Princeton University Press, Princeton, NJ, 1979), p. 121.
[5] W. Greiner, *Quantum Mechanics: An Introduction* (Springer, New York, 1994), p. 282.
[6] P. A. M. Dirac, Proc. R. Soc. Lond. A **114**, 243 (1927).
[7] L. I. Schiff, *Quantum Mechanics* (McGraw-Hill, New York, 1955).
[8] M. L. Goldberger and K. M. Watson, *Collision Theory* (Wiley, New York, 1965).
[9] R. G. Newton, *Scattering Theory of Waves and Particles* (Springer, New York, 1982).
[10] J. R. Taylor, *Scattering Theory: The Quantum Theory of Non-Relativistic Collisions* (Dover, New York, 2006).
[11] M. Iinuma et al., Phys. Lett. A **346**, 255 (2005).
[12] H. Lehman, K. Symanzik, and W. Zimmermann, Nuovo Cimento **1**, 205 (1955).
[13] F. Low, Phys. Rev. **97**, 1392 (1955).
[14] K. Ishikawa and T. Shimomura, Prog. Theor. Phys. **114**, 1201 (2005) [arXiv:0508303 [hep-ph]] [Search INSPIRE].
[15] K. Ishikawa and Y. Tobita, Prog. Theor. Phys. **122**, 1111 (2009) [arXiv:0906.3938 [quant-ph]].
[16] K. Ishikawa and Y. Tobita, AIP Conf. Proc. **1016**, 329 (2008) [arXiv:0801.3124 [hep-ph]] [Search INSPIRE].
[17] K. Ishikawa and Y. Tobita, [arXiv:1106.4968] [hep-ph].
[18] B. Kayser, Phys. Rev. D **24**, 110 (1981).
[19] C. Giunti, C. W. Kim, and U. W. Lee, Phys. Rev. D **44**, 3635 (1991).
[20] S. Nussinov, Phys. Lett. B **63**, 201 (1976).
[21] K. Kiers, S. Nussinov, and N. Weiss, Phys. Rev. D **53**, 537 (1996) [arXiv:9506271 [hep-ph]] [Search INSPIRE].
[22] L. Stodolsky, Phys. Rev. D **58**, 036006 (1998) [arXiv:9802387 [hep-ph]] [Search INSPIRE].
[23] H. J. Lipkin, Phys. Lett. B **642**, 366 (2006) [arXiv:0505141 [hep-ph]] [Search INSPIRE].
[24] E. K. Akhmedov, J. High Energy Phys. **0709**, 116 (2007) [arXiv:0706.1216 [hep-ph]] [Search INSPIRE].
[25] A. Asahara, K. Ishikawa, T. Shimomura, and T. Yabuki, Prog. Theor. Phys. **113**, 385 (2005) [arXiv:0406141 [hep-ph]] [Search INSPIRE].
[26] T. Yabuki and K. Ishikawa, Prog. Theor. Phys. **108**, 347 (2002).
[27] H. L. Anderson et al., Phys. Rev. **119**, 2050 (1960).
[28] K. Homma, D. Habs, and T. Tajima, Appl. Phys. B **106**, 229 (2012).
[29] T. Tajima and K. Homma, Int. J. Mod. Phys. A **27**, 1230027 (2012).
[30] C. H. Lai, "Neutrino electron plasma instability," *Ph.D. Thesis*, University of Texas, Austin (1994).
[31] T. Tajima and K. Shibata, *Plasma Astrophysics* (Addison-Wesley, Reading, MA, 1997), p. 451.
[32] L. Landau, Sov. Phys. Doclady **60**, 207 (1948).
[33] C. N. Yang, Phys. Rev. **77**, 242 (1950).
[34] H. Fukuda and Y. Miyamoto, Prog. Theor. Phys. **4**, 49 (1949).

[35] J. Steinberger, Phys. Rev. **76**, 1180 (1949).
[36] L. Rosenberg, Phys. Rev. **129**, 2786 (1963).
[37] S. L. Adler, Phys. Rev. **177**, 2426 (1969).
[38] J. Liu, Phys. Rev. D **44**, 2879 (1991).
[39] R. P. Feynman, Phys. Rev. **76**, 749 (1949).
[40] A. I. Alelseev, Zh. Eksp. Teor. Fiz. **34**, 1195 (1958) [Sov. Phys. JETP **7**, 826 (1958)].
[41] K. A. Tumanov, Zh. Eksp. Teor. Fiz. **25**, 385 (1953).
[42] T. Tajima and J. M. Dawson, Phys. Rev. Lett. **43**, 267 (1979).
[43] R. Barbieri, R. Gatto, and R. Kogerler, Phys. Lett. B **60**, 183 (1976).
[44] W. Kwong, P. B. Mackenzie, R. Rosenfeld, and J. L. Rosner, Phys. Rev. D **37**, 3210 (1988).
[45] Z. P. Li, F. E. Close, and T. Barns, Phys. Rev. D **43**, 2161 (1991).
[46] G. T. Bodwin, E. Braaten, and G. P. Lepage, Phys. Rev. D **51**, 1125 (1995).
[47] H. W. Huang and K. T. Chao, Phys. Rev. D **54**, 6850 (1996).
[48] J. E. Gaiser et al., Phys. Rev. D **34**, 711 (1986).
[49] S. B. Athar et al., Phys. Rev. D **70**, 112002 (2004).
[50] M. Ablikin et al., Phys. Rev. D **71**, 092002 (2005).
[51] J. Beringer et al. (Particle Data Group), Phys. Rev. D **86**, 010001 (2012).
[52] M. Gell-Mann, Phys. Rev. Lett. **6**, 70 (1961).
[53] K. Ishikawa and Y. Tobita, JPS Conf. Proc. **1**, 013010 (2014).
[54] Y. Inoue et al., Phys. Lett. B **668**, 93 (2008).
[55] J. Arafune and G. Takeda, *Total Reflection of Relic Neutrinos from Material Targets*, University of Tokyo, ICEPP Report, ut-icepp 08-02, unpublished.
[56] M. G. Aartsen et al. (IceCube Collaboration), [arXiv:1405.5303 [astro-ph.HE]] [Search INSPIRE].
[57] P. Abreu et al. (Pierre Auger Collaboration), Adv. High Energy Phys. **2013**, 708680 (2013) [arXiv:1304.1630 [astro-ph.HE]] [Search INSPIRE].
[58] G. I. Rubtsov et al. (Telescope Array Collaboration), J. Phys. Conf. Ser. **409**, 012087 (2013).
[59] R. C. Franz, R. J. Nemzek, and J. R. Winckler, Science **249** 48 (1990).
[60] G. J. Smith et al., Science **264**, 1313 (1994).
[61] T. Torii, M. Takeishi, and T. Hosono, J. Geophys. Res. **107**, 4324 (2002).
[62] H. Tsuchiya et al., Phys. Rev. Lett. **99**, 165002 (2007).
[63] T. Tajima, S. Cable, K. Shibata, and R. M. Kulsrud, Astrophys. J. **390**, 309 (1992).
[64] C. Cohen-Tannoudji, J. Dupont-Roc, and G. Grynberg, *Photons and Atoms: Introduction to Quantum Electrodynamics* (Wiley, New York, 1989).